



VCU

Virginia Commonwealth University
VCU Scholars Compass

Theses and Dissertations

Graduate School

2015

The Effect of Optogenetic Manipulation of SS interneurons within Malformed, Epileptogenic Cortex

Nicole Ekanem
Virginia Commonwealth University

Follow this and additional works at: <https://scholarscompass.vcu.edu/etd>



Part of the [Nervous System Diseases Commons](#)

© The Author

Downloaded from

<https://scholarscompass.vcu.edu/etd/3990>

This Thesis is brought to you for free and open access by the Graduate School at VCU Scholars Compass. It has been accepted for inclusion in Theses and Dissertations by an authorized administrator of VCU Scholars Compass. For more information, please contact libcompass@vcu.edu.

© Nicole Ekanem 2015

All Rights Reserved

**THE EFFECT OF OPTOGENETIC MANIPULATION OF SS INTERNEURONS
WITHIN MALFORMED, EPILEPTOGENIC CORTEX**

A thesis submitted in partial fulfillment of the requirements for the degree of Master of Science
at Virginia Commonwealth University

by

Nicole Ekanem
B.S. Virginia Commonwealth University, 2012

Director: Kimberle Jacobs, Ph.D.
Associate Professor
Department of Anatomy and Neurobiology

Virginia Commonwealth University
Richmond, Virginia
August, 2015

Acknowledgement

I would like to thank fellow lab members for their assistance with the completion of this work: thanks to Laura Reed for her help with whole cell recordings, Olivia Bowles for performing the utilized NeuN staining, Nicki Weston for breeding the mice and performing the freeze lesion surgeries, and Nigal Shah and Chris Conrad for their help with the non-optogenetic field experiments. Additional thanks to my committee, my family, and everyone else who had the audacity to bear with me during the completion of this work! And of course, thanks to Dr. Kimberle Jacobs for the opportunity. May this forever serve as a personal reminder to take of my business in a timely, organized manner and to maybe not depend so much on café lattes over sleep...

Table of Contents

List of Figures.....	v
List of Abbreviations and Definitions.....	vii
Abstract.....	1
Chapter 1 Introduction.....	3
1.1 Epilepsy.....	3
1.2 Intractable nature of some epilepsies; intro to cortical malformations..	4
1.3 Polymicrogyria.....	6
1.4 Animal model of polymicrogyria.....	8
1.5 Neocortical interneurons.....	15
1.6 Optogenetics	22
Chapter 2 Optogenetic manipulation of SS interneurons	32
2.1 Hypothesis and objectives.....	32
2.2 Materials and Methods.....	33
Chapter 3 Results.....	39
3.1 Freeze lesion in P1 mouse is similar to P1 rat	39
3.2 Freeze lesion at P1 produces epileptiform activity w/in PMR	40
3.3 SS interneuron activation effect on evoked field potentials	40
3.4 Pyramidal and SS-LTS neuron identification	41
3.5 The effect of SS-ChR2 activation in pyramidal neurons	43
3.6 The effect of SS-Arch silencing in pyramidal neurons	49
3.7 Results summary.....	50
Chapter 4 Discussion.....	66
List of References	77
Vita.....	88

List of Figures

Figure 1.1	Graphic: SS and PV inhibition as it differs between control and PMR cortex.....	31
Figure 2.1	Primary Somatosensory Cortex [Allen Brain atlas].....	38
Figure 3.1	NeuN stained images of microgyria and lamination patterns therein	52
Figure 3.2	Field potential epileptiform activity.....	54
Figure 3.3	Effect of bLED on evoked field potentials	55
Figure 3.4	Pyramidal and SS/LTS interneuron images and intrinsic properties	56
Figure 3.5	SS-ChR2 interneuron responsiveness to bLED	57
Figure 3.6	SS interneuron evoked pyramidal neuron IPSCs.....	58
Figure 3.7	Assessment of SS interneuron probability of release	59
Figure 3.8	Comparison of SS interneuron induced inhibition from lateral distances	60
Figure 3.9	Comparison of SS interneuron induced inhibition from lateral distances	61
Figure 3.10	Comparison of SS interneuron induced inhibition from superficial layers	62
Figure 3.11	Effect of SS interneuron activation on evoked pyramidal neuron IPSCs.....	63

Figure 3.12	SS-Arch interneuron responsiveness to yLED	64
Figure 3.13	Effect of SS interneuron silencing on spontaneous IPSCs	65
Figure 4.1	Model visualizing synaptic relationships between SS, PV, and Pyr.....	75
Figure 4.2	Induction of epileptiform activity with bLED	76

List of Abbreviations and Definitions

°C	degrees Celsius
aCSF	artificial cerebrospinal fluid
AED	antiepileptic drugs
AMPA(R)	glutamate receptor
Arch	archaerhodopsin
APV	NMDA receptor antagonist
CAMKII	Ca ²⁺ /calmodulin-dependent protein kinase II
CNS	central nervous system
ChR	channelrhodopsin
Cre	Cre recombinase; enzyme
Cre- <i>lox</i>	Cre- <i>lox</i> recombination; site-specific genetic recombination technique
DIC	Differential interference contrast; optical microscopy illumination technique
DNQX	AMPA receptor antagonist
E/I	excitation/inhibition; ratio
EPSC	excitatory postsynaptic current
eEPSC	evoked EPSC
mEPSC	miniature EPSC; postsynaptic response to neurotransmitter released by single presynaptic vesicle
sEPSC	spontaneous EPSC
FS	fast spiking
GABA	γ-aminobutyric acid
GFP	green fluorescent protein
IPSC	inhibitory postsynaptic current

eIPSC	evoked IPSC
mIPSC	miniature IPSC; postsynaptic response to neurotransmitter released by single presynaptic vesicle
sIPSC	spontaneous IPSC
IPSP	inhibitory postsynaptic potential
LTS	low threshold spiking
mGluR	metabotropic glutamate receptor
mM	milli-Molar
mOsm	milli-Osmole
NMDA(R)	glutamate receptor
NR2B	NMDAR subunit
P	postnatal day
PMR	paramicrogyral region
PV	parvalbumin
SS	somatostatin
μm	micrometer
μM	micro-Molar
VB	ventrobasal complex of thalamus
VIP	vasoactive intestinal peptide
YFP	yellow fluorescent protein

ABSTRACT

The Effect of Optogenetic Manipulation of SS interneurons within Malformed, Epileptogenic Cortex

By Nicole Ekanem

A thesis submitted in partial fulfillment of the requirements for the degree of Master of Science in Anatomy and Neurobiology at Virginia Commonwealth University

Virginia Commonwealth University, 2015.

Advisor: Kimberle M Jacobs, Ph.D.
Associate Professor, Department of Anatomy and Neurobiology

A large percentage of individuals with intractable epilepsies have an accompanying cortical malformation, the underlying cellular mechanisms of which are poorly understood. It is known however that in an animal model for one such malformation, polymicrogyria, epileptogenesis occurs most easily from an adjacent area termed the paramicrogyral region (PMR). Previous studies implicate SS interneurons as a potential contributor to this pathology, which lead to our hypothesis: in PMR, SS interneurons exert a higher modulatory influence on excitatory pyramidal cells, as compared to the same by SS interneurons within homologous control cortex.

Using a freeze-lesion model for polymicrogyria in transgenic mice that selectively express either Channelrhodopsin or Archaelhodopsin optogenetic channels in these cells, we assessed the contribution of SS interneurons as it potentially differs between layer V of PMR and control cortex. These studies provided the following biological examples in support of previous extrapolations that indicate SS over-activation within PMR: (1) SS interneuron mediated evocation of inhibitory events in layer V excitatory neurons is more robust in PMR than in

control. Similarly, electrically-evoked inhibitory events in these excitatory neurons trend towards being larger, signifying a larger contribution by interneurons. (2) SS interneuron mediated suppression of electrically-evoked responses trends towards being stronger in PMR; and (3) the selective silencing of SS interneurons might not impart an effect on spontaneous inhibitory postsynaptic events.

Chapter 1

Introduction to Epilepsy, Interneurons, and Optogenetics

1.1 Epilepsy

Epilepsy, previously classified through folklore as a sign of a divine religious experience or demonic possession, has since lost its “sacred quality” through slow discovery that has steadily revealed more about its clinical nature (Eadie and Bladin 2001). From its earliest known reference in the ancient Babylonian medical text, *Sakikku* (Eadie and Bladin 2001), all the way to John Hughlings Jackson and his seminal epilepsy research in the mid-1800s (Balcells 1999), epilepsy is now defined as a grouping of neurological disorders characterized symptomatically by recurrent and spontaneous epileptic seizures. At the time of this writing, a number of different epilepsies of genetic or acquired etiologies have been characterized and explicated (Bladin et al. 2000; Frey 2003; Hayashi et al. 2002; Sedel et al. 2007); however, many individuals are still spate with epilepsies that are poorly understood and consequently unmanageable, despite diagnostic and treatment advancements (Schuele and Luders 2008). Undoubtedly, there is still very much to be revealed about this syndrome and its underlying mechanisms.

Symptomatically, epilepsy can be debilitating. As briefly stated above, individuals with this disorder experience multiple, recurrent, and spontaneous seizures, the clinical representation of excessive and hypersynchronous neuronal firing. An epileptic seizure can take many forms, the severity and type of which depend on location and spread of neural area exhibiting this pathological synchronicity. Two seizure categories have been instituted by the Commission on Classification and Terminology of the International League against Epilepsy (*Epilepsia* 1989).

The first, partial seizures, comprise abnormal neuronal activity restricted to a focal region of the brain. Symptoms, thereby, may involve a specific motor or sensory experience, occurring in the absence of proper external stimulus. The second generalized seizures, may yield a more severe presentation as both hemispheres tend to be involved—loss of consciousness, and abnormal postural muscle tone fall under this category; patients may even collapse upon the generation of this type of seizure.

With relatively high world-wide prevalence (7%; World Health Organization website, www.who.int/en) and a high proportional incidence in patients during the extremes of life (neonatal and post 70 years of age; Hauser 1998), the importance of clinical and basic science research in this field is clear. In fact, because of modern diagnostic techniques, numerous and diverse etiologies for these disorders have been identified. These include: genetic predisposition, traumatic brain injury, tumor, congenital disease, infectious disease of the central nervous system (CNS) and developmental malformations (Bladin et al. 2000; Berkovic et al. 2006; Jallon et al. 2001; Leventer et al. 2008; Mirski and Varelas 2008). Developmental malformations typically result in abnormal cortical lamination, also called cortical dysplasia. These are of particular interest since they previously went unrecognized prior to the development of modern imaging techniques (Barkovich et al. 1999; Hayashi et al. 2002; Lim et al. 2005; Takanashi et al. 2006).

1.2 Intractable nature of some epilepsies and introduction to cortical malformations

Currently available treatment options are sufficient to alleviate symptoms for the majority of individuals with epilepsy. Antiepileptic drugs (AEDs), the most commonly used, however, do not offer relief for 30-40% of total patients (Kwan and Brodie 2006). Of this long-suffering group, many of whom express an epilepsy etiologically tied to a cortical malformation (Guerrini

and Carrozzo 2002), alternative non-pharmacological interventions, such as vagal nerve stimulation and ketogenic diets, are only effective in a small minority (Dua et al. 2005). Surgical resection is an additional option for individuals within this etiologic group when the seizure origin is focally restricted to one hemisphere, clearly differentiated from eloquent cortex, and not complicated by additional hindrances (Blumcke et al. 2009; Sisodiya 2000). Even so, symptoms return in about 40% of these individuals (Sisodiya 2000). This phenomenon is attributed mainly to limited electroencephalography (EEG) and electrocorticography (ECoG, intracranial EEG) spatial resolution which impedes a physician's ability to accurately delineate the epileptogenic, or seizure originating region, not to mention the potential for widespread, epilepsy-promoting abnormalities extending beyond the aforementioned locus (Sisodiya 2000). Polymicrogyria is an example of an epilepsy-promoting cortical malformation that has limited potential for both AED intervention and symptom amelioration after surgical resection (Sisodiya 2004).

Developmental malformations, as a class, are a common cause of intractable epilepsies, especially in children (Flint and Kriegstein 1997; Wyllie 2000). Abnormalities of development such as this may result from errors that occur any time during the development of the CNS. Errors too early may inhibit the generation of cells, or cause too many cells to die, while disruptions occurring at later stages may result in improper migration of cells (Barkovich and Kjos 1992; Guerrini et al. 2003).

These are just a few examples in a sundry of different varieties, spanning a vast array of severities and inducing factors. This writing will focus on polymicrogyria, a type of developmental malformation, and its epilepsy-promoting characteristics.

1.3 Polymicrogyria

One of the more common cortical dysplasias, polymicrogyria, is identifiable through magnetic resonance imaging of characteristic disproportionate and abnormally small cortical gyrations on the surface of the brain, lending it an irregular, bumpy appearance (Barkovich 2010; Sisodiya 2004). It is produced by a specifically timed error or disruption in cortical development. The inciting disruption can be varied, but may involve a genetic mutation (Lee et al. 1997), be acquired in utero via ischemic (Barkovich 2010; Dvorak and Feit 1977) or infectious insult (Montenegro et al. 2002), or even by abdominal trauma during pregnancy (Montenegro et al. 2002). Recent momentum in the advancement of medical imaging has etiologically linked this malformation with epilepsies previously considered idiopathic (Barkovich and Kjos 1992); Hauser 1998; Lim et al. 2005; Takanashi et al. 2006).

This malformation type has two defined histological presentations. The first, unlayered polymicrogyria, is caused by an early disruption of neuronal migration—early, relative to the timing that induces the second histological type. This malformation presents with an external molecular layer that does not follow the normal pattern of convolutions, overtop a region of underlying neurons that lack laminar organization (Guerrini and Carrozzo 2002). The second type, four-layered polymicrogyria, follows an insult that occurs between the 20th and 24th week of gestation (Guerrini and Carrozzo 2002). As per its name, this type presents as a focal 4-layered region, which contrasts with typical 6-layered neocortex (Guerrini and Filippi 2005). Given the presence of intracortical laminar necrosis within these malformations (Guerrini and Filippi 2005; Montenegro et al. 2002), it has been inferred that an inciting event, such as in utero ischemia during the aforementioned time windows, will generate such dysplasias by causing the death of deep cortical layers. At this stage, since the brain is developing inside-out (layers deep

to pia forming before superficial) an insult during migration will effectively remove deep layers; superficially directed layers migrate into that space heterotopically (Rakic and Lombroso 1998).

As revealed by Jacobs et al. in 1999, the epileptogenic, or seizure-initiating site in a patient with this type of malformation might not always solely involve the visibly lesioned tissue itself, but rather extend beyond and involve the cortical area adjacent to it (Chassoux et al. 2008; Jacobs et al. 1999a). This confounds the ability to assign boundaries to and surgically resect the seizure-initiating areas to success, since the epileptogenic portions of cortex surrounding the obvious malformation otherwise appear to be eloquent cortex (Araujo et al. 2006; Chassoux et al. 2008). Additionally, neurons within the malformation proper have been shown to activate during the induction of motor activity and language (in individuals where polymicrogyric cortex was within areas corresponding to the motor strip or Broca's area, respectively; Araujo et al. 2006). Such functionality hinders surgical success even further as removal of these areas without careful functional planning could prompt the development of new symptoms in a patient (Araujo et al. 2006).

Pinpointing an alternative treatment target for individuals with this malformation is essential, as many of them live ensnared by its many clinical manifestations, which can include: severe encephalopathy, cognitive impairments, spastic paresis, and as mentioned, intractable seizures (Araujo et al. 2006; Guerrini and Carrozzo 2002). Work in this correspondence will utilize an animal model of human polymicrogyria to study epilepsy-promoting cellular mechanisms within epileptogenic areas adjacent to microgyric tissue, which at the time of this writing, still remain poorly understood.

1.4 Animal model of microgyria

1.4.1 Background and freeze-lesion methodology

In the late 70s, the Dvorak lab developed an animal model that produces, in rodents, similar histopathology expressed by human four-layered polymicrogyria (Dvorak and Feit 1977; Dvorak et al. 1978). Their methodology calls for the placement of a freezing probe (-100°C) onto the skull of a neonatal rat pup for a duration of one to two and a half seconds, creating a transcranial ischemic lesion (Dvorak and Feit 1977; Dvorak et al. 1978). Rats are born at a developmental stage equivalent to the 18th to 24th gestational week in humans, a developmental phase during which cortical neuroblast migration is taking place (Dvorak and Feit 1977; Humphreys et al. 1991). Neuronal migration, occurring in a deep to superficial stereotype, is not complete at this juncture; therefore, contact freezing during this period will thrombose blood vessels and cause the necrosis of neurons present on the cortical plate, which at this period of cortical development, comprise layers IV, V, and VIa (Dvorak and Feit 1977). Migration of superficially-intended neuroblasts and capillaries will continue, resulting in a focal microgyric region of dyslaminated cortex containing four layers, instead the six typically seen in neocortex (Dvorak and Feit 1977). This focal region occupies about one to four millimeters coronally if induced by a 2 X 5 millimeter rectangular freezing probe. The generated microgyrus possesses a superficial aspect, denoted with Arabic numerals (Jacobs et al. 1999b) as layers 1 and 2. Layers 1 and 2 are anatomically similar to normal neocortical layers I and II/III and are continuous with them, respectively (Crome 1952; de Leon 1972; Dvorak and Feit 1977; Humphreys et al. 1991; Jacobs et al. 1996; Rosen et al. 1996). Layer 3 is thin with a small population of glia-resembling cells with small somata (Dvorak and Feit 1977) that terminates abruptly at the site where microgyrus and adjacent six-layered cortex meet (Crome 1952; de Leon 1972). Layer 4 is similar

to and often contiguous with layer IVb of normal cortex (Crome 1952; de Leon 1972; Dvorak et al. 1978 ; Jacobs et al. 1996).

The timing of lesion induction is critical for the maintenance of this model. Jacobs et al. demonstrated that rats lesioned at postnatal day (P) 1 consistently exhibit hyperexcitability, a critical component in epileptogenesis, well into adulthood. Animals lesioned earlier at P0 displayed a decreased incidence in epileptiform responses following age P40 (Jacobs et al. 1999a). Similarly, Kellinghaus et al. found no difference in the amount of cortical excitability in adult (P60) rats that were lesioned at P0 compared to non-lesioned rats of that same age (Kellinghaus et al. 2007). Evidently, a lesion induced too early in cortical development results in amelioration of the generated pathology with time. Further, Dvorak et al. demonstrated that this same lesion performed on rats at P4 would not induce a microgyric malformation, once again adding credence to the time-specificity, or critical period, required for an inciting error to result in anomalous layering (Dvorak et al. 1978).

Freeze-lesioned rats are not known to experience spontaneous seizures, but are prone to exhibit epileptiform activity associated with the induced microgyrus (Barkovich and Kjos 1992; Jacobs et al. 1999a; Scantlebury et al. 2004). The occurrence of epileptiform activity within slices from these animals has been demonstrated consistently and reproducibly at P12, a developmental age wherein neural development is similar to that in humans at birth. Correspondingly, polymicrogyria-associated seizures may begin in newborns at birth or be delayed for years (Fasulo et al. 2012; Pascual-Castroviejo et al. 2001). Epileptiform activity itself is generated from a cortical expanse directly adjacent to the microgyrus proper, termed the paramicrogyral region (PMR; Jacobs et al. 1996). This hyperexcitable area offers researchers a unique and helpful perspective, allowing for suitable evaluation of the hyperexcitable brain's

proclivity to induce seizure. As will be discussed in more detail below, the onset timings of hyperexcitability and epileptogenicity within this region are delayed and staggered. Researchers can study the PMR to reveal particular alterations that might occur before the area becomes hyperexcitable, and similarly, before epileptogenesis. Therefore, this animal model, wherein rodents are freeze lesioned at P1 is an accepted and robust method for the study of the epileptogenic mechanisms inherent to human polymicrogyria.

Studies in this communication will take place within epileptogenic PMR, since this area, being sensitive to the generation of epileptiform activity, is an advantageous place to look for epileptogenic mechanisms. Cellular and subcellular characteristics of the model, as they pertain to the induction of epileptiform activity, will be delineated in the following sections.

1.4.2 Cellular and sub-cellular characteristics of freeze-lesion model

Studies focused on identifying the cellular characteristics inherent to this freeze-lesion model have revealed that neurons within the microgyrus are not generated in response to the lesion (Rosen et al. 1996), but instead, are prenatally generated, and migrate through or around the damaged area to reach their final station. One study demonstrated that cell-dense layer 2 within the microgyrus contains neurons generated between embryonic days 17 through 20, which would normally end up occupying layers III and IV in eloquent neocortex (Rosen et al. 1996). Neurons formed earlier at embryonic day 15 were not found in the microgyrus; a significant find, since these neurons would have inhabited the deep neocortical layers (Dvorak and Feit 1977; Rosen et al. 1996). This is consistent with this model's mechanism of ischemia-induced cell death selective to deep-layer neurons. Nissl staining of sections taken from rats aged P21 and P60 demonstrate that local neurons are morphologically normal within these areas, while glial

fibrillary acidic protein and glutamate staining reveal widespread disorder of neocortical architecture (Humphreys et al. 1991). Neurofilament staining is scarce within the microgyrus, but overabundant in the PMR, as compared to homologous control (Humphreys et al. 1991). This suggests the potential for the preservation of excitatory processes, originally aimed at the microgyrus, that would otherwise have been eliminated given the loss of their intended destination (Jacobs et al. 1999; Humphreys et al. 1991). Further, it has been suggested that the cortical region containing the microgyria proper is 'dysmature' or delayed developmentally, as indicated by the persistence of elements that are typically eliminated early in non-injured cortex (Cepeda et al. 2006). One example of this are normally transitory Cajal-Retzius cells, which are present in P12 rat PMR cortex, but absent in control tissue by this postnatal age (Super et al. 1997). Additionally, fibers resembling radial glia have been observed within lesioned cortex up to the fifth postnatal week; in non-injured cortex, these elements are not present by this point in development (Rosen et al. 1992).

This model also prompts numerous subcellular alterations, primarily involving receptor subunit expression. In regard to inhibitory GABA_A receptor expression, two of its subunits, $\alpha 2$ and $\alpha 3$, are normally considered premature and replaced in the second postnatal week with $\alpha 1$ or $\alpha 4$ (Laurie et al. 1992). Immunohistochemical staining for individual GABA_A receptor subunits medial and lateral to freeze-lesioned microgyrus by Redecker et al, revealed a decrease in all subunits, except for $\alpha 3$, again, known to decrease in expression as development ensues (Redecker et al. 2000). Another group demonstrated similarly that (premature) $\alpha 2$ and $\alpha 3$ subunit expression persists within PMR, at the expense of $\alpha 1$ (Defazio and Hablitz 1999). This may be a contributing factor to another observed phenomenon where decreased binding to GABA_A receptors occurs in regions of cortex surrounding the lesion (PMR), with binding levels reaching

normalcy outside of this range (Zilles et al. 1998). Taken together, these findings suggest not only that there is altered expression of inhibitory GABA_A receptor within freeze-lesion induced PMR, but that there may also be reduced receptor density.

Excitatory glutamate receptors also appear to be changed in this model. For instance, increases in AMPA and kainite receptor binding have been demonstrated (Zilles et al. 1998) and enhanced functioning of NR2B subunit containing NMDA receptors has been demonstrated (Defazio and Hablitz 2000). Persistence of NR2B subunit, typically expressed in the embryonic brain, also supports previous claims of a dysmature (Cepeda et al. 2006) microgyral cortex.

1.4.3 Altered anatomical and functional connectivity and introduction to hyperexcitability

Anatomical connectivity to, within, and from microgyria and adjacent PMR have been demonstrated via the injection of neuronal tracers into the microgyrus proper, ipsilateral and contralateral homotopic regions in control brain, and thalamus (Giannetti et al. 1999; Giannetti et al. 2000). Studies of this nature disclose that local pyramidal cell afferents and commissural fibers are organized abnormally within microgyrus and around it in corresponding PMR (Giannetti et al. 2000). Additionally, some thalamic nuclei as well as efferent thalamocortical fibers from them, undergo important alterations. One particular thalamic site, the ventrobasal complex (VB), which normally conveys direct connections to the somatosensory cortex, has fewer neurons in animals with a lesion in this region (Rosen et al. 2006). It seems the presence of microgyria here yields a reduction in VB targeting area, prompting the VB to reroute efferents and hyperinnervate adjacent PMR (Rosen et al. 2000). This is supported with cytochrome oxidase (CO) staining in these areas, which is greatly increased in microgyria-surrounding PMR,

but decreased within the microgyria itself (Jacobs et al. 1999c). These efferents are traditionally excitatory in their influence as afferents to their respective cortical targets.

Functionally, the consequences of hyperinnervation within PMR by thalamocortical afferents are varied. One corollary of note is a general increased level of miniature excitatory postsynaptic current (mEPSC) activity in pyramidal neurons within layer V of PMR, as compared to the same within layer V of homologous control cortex (Jacobs and Prince 2005; mEPSC defined in appendix). This indicates that excitatory afferents are not only structurally increased, but functionally increased as well. Second, spontaneous excitatory postsynaptic current (sEPSC) and mEPSC frequencies have also been shown to rise incrementally in rats, from pre-epileptogenic ages P7 to P11 (Zsombok and Jacobs 2007), on top of mEPSC levels already being high in PMR (Jacobs and Prince 2005). This young age group precedes the age at which epileptiform activity can be evoked (P12; Jacobs et al. 1999), suggesting that this incremental s/mEPSC increase may contribute in some way to the onset of epileptogenesis. The mEPSC increase in this age group supports not only the premise that an increased number of excitatory afferents may exist in the PMR, but also brings up the possibility of an increased release probability from these neurons (Zsombok and Jacobs 2005). A third type of EPSC, evoked (ePSC), are multip peaked, have larger amplitudes, and greater area in PMR, further evidencing the presence of increased excitatory input to the PMR. All of this together implies that functional excitability is increased within the PMR; this PMR-inherent hyperexcitability has been demonstrated to exist all the way up to P118 (animals older than P118 were not analyzed; Jacobs et al. 1996). Delineation of hyperexcitable PMR was accomplished by field potential studies, where stimulation of cortex at a distance of 0.5 mm to 2 mm away from the microgyrus, but no further, resulted in evoked epileptiform activity (Jacobs et al. 1999; Luhmann et al. 1998).

Epileptogenic mechanisms, including hyperexcitability, therefore exist primarily within this area. Epileptogenic alterations within PMR are resilient and do not depend on the microgyria proper as resection of the lesion itself has not been shown to ameliorate the ability to evoke epileptiform activity from this area (Jacobs et al. 1999a).

In addition to alterations with excitatory circuitry discussed above, functional changes as induced by hyperinnervation of thalamocortical afferents within the PMR also involve inhibitory circuitry. Evoked inhibitory postsynaptic currents (eIPSCs) have been shown to be enhanced for a subset of pyramidal cells in layer V of lesioned cortex, a response that is diminished back to control values upon bath application of APV and DNQX, respective NMDA and AMPA receptor antagonists (Jacobs and Prince 2005). This indicates that the enhanced excitatory input reaches inhibitory cells as well as excitatory ones. Miniature (m)IPSC frequency was not shown to be altered in PMR, which suggests a maintained number of inhibitory synapses, assuming release probability is preserved at these terminals (Jacobs and Prince 2005). At the same time, another study has alternatively demonstrated a decrease in inhibitory post synaptic potential (IPSP) conductance within layer II/III pyramidal neurons in PMR (Luhmann et al. 1998). In this same vein, a reduction in the number of immunoreactive cells of a certain inhibitory GABAergic interneuron subpopulation has been demonstrated (Jacobs and Prince 2005). What these contradictions potentially mean for the inhibitory network, as impaired in the lesioned brain, will be discussed at length in subsequent sections.

1.4.4 Involvement of interneurons in epilepsy-promoting characteristics of microgyria

Intuitively, epilepsy, as induced by hyperexcitable PMR cortex in this model, should be causally linked to the increased excitatory afferentation and enhanced glutamatergic receptor

binding and functioning (Jacobs et al. 1999c; Jacobs and Prince 2005; Zsombok and Jacobs 2007). This has been demonstrated consistently and reproducibly over the years. However, and as introduced above, there is further evidence implicating both excitatory and inhibitory networks (Jacobs et al. 1999). Lines of evidence submit that increased excitation alone cannot account for PMR hyperexcitability, including the demonstrated delay that occurs between the increase in excitatory input to PMR pyramidal cells and the later onset of epileptogenesis (Jacobs et al. 1999a; Zsombok and Jacobs 2007). Further, increased excitatory input to at least some inhibitory targets has been established (Jacobs and Prince 2005), which supports the possibility that enhanced and not diminished inhibitory function, may play a critical role in the pathophysiology of epileptogenesis (Klaassen et al. 2006; Mann and Mody 2008; Prince and Jacobs 1998). The experiments described in this communication focus on one neocortical interneuron subtype that has been implicated mechanistically in such a way by previous studies for the purpose of confirming whether or not it imparts a grander epileptiform activity-promoting influence in PMR cortex, as compared to its influence in control cortex.

1.5 Neocortical interneurons

1.5.1 Background

In concept, the interneuron has until recently managed to maintain indefinability. As a term, it was originally used to modestly define cells existing between input and output neurons in invertebrates (Maccaferri and Lacaille 2003). Though, once the notion of inhibition was described, interneuron became instead, the categorical name for inhibitory cells that share space with, but exist in structural and functional contrast to, excitatory principal cells (Maccaferri and Lacaille 2003). These cells, exhibiting immense variations among their morphological,

electrophysiological, molecular, and synaptic characteristics, account for 20-30% of the total neocortical cell population (Markram et al. 2004; Houser et al. 1983). Nevertheless, unifying features for neocortical interneurons do exist, namely excitatory glutamate being supplanted by inhibitory γ -aminobutyric acid (GABA), a neocortical interneuron's primary neurotransmitter. Interneurons lack long-distance apical dendrites or dendritic spines characteristic to pyramidal cells (Markram et al. 2004), and instead, possess short axons that tend not to project beyond cortex into white matter or distant brain regions; these rather arborize vertically within a column, or horizontally within lamina. A single interneuron can affect the firing patterns of multiple pyramidal cells by exerting a rhythmic modulatory influence upon them, inducing neuronal synchrony (Colmers and El Bahh 2003). Synchrony, or the act of pyramidal cells firing in unison at regular intervals, as it physiologically occurs in non-impaired cortex, is crucial for the induction of network phenomena such as sensory perception, information processing, formation of representative maps, motor activity, states of consciousness, attention, and more (Fricker and Miles 2001; Singer 1999). However, excessive synchronization, as can occur from unchecked overexertion of inhibitory neurons, can induce an epileptic seizure (Van Quyen et al. 2003).

Alterations in these local inhibitory circuits can and do occur in an impaired brain, causing imbalance between cortical excitation and inhibition (E/I). In fact, many psychological disorders are a consequence of such imbalance; these include: schizophrenia, autism spectrum disorder, and intellectual disability (Dichter and Ayala 1987; Marin 2012). How each type of interneuron contributes to its local modulatory network is a direct consequence of their respective morphological, intrinsic, molecular, and synaptic characteristics. Combinations of these characteristics, together, allow for accurate cellular identification and classification; this way, their functional relationships and potential pathologies, may be delineated in a more useful

manner. The subsequent section is a condensed summary of popularly utilized methods for cortical interneuron characterization.

1.5.2 Interneuron subtype morphology, electrophysiology and molecular markers

Interneurons are morphologically dissimilar in many ways; the extent of their respective axonal arbors, varying shapes and laminar positions of cell somata, and shapes of dendritic trees are a few commonly delineated distinctions (*Cerebral Cortex* 1984). Groupings can be further distinguished in terms of arbor orientation. Certain cells possess arbor with intracolumnar, or vertically-spanning dendrites, while others are intralaminar or horizontally-spanning. Perpendicular in their influence, cells that fall under these categories hold obvious functional differences. One type of vertically-oriented interneuron, the Martinotti cell, has somata that originate in layers II through VI; its axons ascend to layer I, wherefrom they arborize horizontally and synapse onto the distal tuft dendrites of pyramidal cells (Wang et al. 2004; Fairen et al. 1984; Markram et al. 2004). Some others, bitufted, bipolar, and double-bouquet are all oriented vertically as well, but differ in their cortical distributions, cellular targets, somal size, and arbor densities (Fairen et al. 1984; Markram et al. 2004). These vertically-oriented cells, and others, possess the capacity to simultaneously inhibit multiple neurons within a column and between cortical lamina. Horizontally-oriented cells, rather synapse on flanking cell bodies residing within the same layer, thereby supplying inhibition within a layer but across columns. An example of such an intralaminar interneuron is the Chandelier cell. These cells are named for their unique spray of horizontal axon branches that form synapses selectively with pyramidal cell axon initial segments (Somogyi 1977). A second type, the basket cell, presents differently throughout the brain. Large basket cells can send axons into bordering columns and synapse onto

the soma of pyramidal cells therein, while small basket cells are densely arborized and only make contacts with neighboring pyramidal cell bodies (Markram et al. 2004; Wang et al. 2002).

Classification can also be made based on intrinsic membrane properties as these cells each fire action potentials in distinctive and predictable patterns (Markram et al. 2004). Of the many known firing configurations, focus will be held on two types: fast-spiking and low threshold-spiking, as they are characteristic of the two main interneuron populations discussed in this work.

Fast-spiking (FS) interneurons, fire a rapid progression of action potentials with little to no adaptation in response to injection of a depolarizing current, while low threshold-spiking (LTS) interneurons respond to the same input with an attenuating progression of action potentials (Kawaguchi 1993; McCormick et al. 1985). Action potentials in FS cells have outstandingly short half-widths of less than one millisecond when compared to that of LTS cells (> one millisecond) (Kawaguchi 1993). Maximum firing frequency is also higher among FS cells (Kawaguchi and Kondo 2002) and action potential afterhyperpolarization period is shorter (Kawaguchi 1993). Additionally, following the application of a hyperpolarizing current, LTS cells have the capacity to fire rebound action potentials upon a return to resting membrane potential (Kawaguchi 1993). Finally, IPSCs recorded from FS cells display faster kinetics and larger amplitudes than those recorded from LTS cells (Bacci et al. 2003).

Molecular markers allow a third way to distinguish interneuron subtypes, as they enable researchers to identify molecular characteristics inherent to certain cortical areas, thus revealing separate, non-overlapping cell type populations. Interneurons selectively express certain proteins and peptides (Kawaguchi and Kubota 1997): Parvalbumin (PV), a calcium-binding protein, as well as Somatostatin (SS) and Vasoactive Intestinal Peptide (VIP), two peptides, are three

cellular markers of note. Each are expressed in cortical layers II/III, V, and VI, but never overlap; this indicates that they likely each correspond to separate cell types. It is also possible for the incidence of a molecule to be correlated with known cell morphology, as it seen with SS and Martinotti cells (Kawaguchi and Kubota 1997; Markram et al. 2004). PV correlates with FS electrophysiology (Cauli et al. 1997; Kawaguchi and Kubota 1993; Kawaguchi and Kubota 1997), and SS with LTS (Gibson et al. 1999). VIP correlates with neither, indicating another interneuron subtype (Markram et al. 2004).

These methods of identification are often used together in an attempt to accurately characterize a cell of one type. Proper identification is paramount especially in the context of how these cells contribute to their respective circuits. Further discussion will involve the circuitry of two interneuron subtypes, which we can identify based on the features listed above, and how they each specifically contribute to their inhibitory cortical networks.

1.5.3 Interneuron circuitry

To consolidate, FS cells, which follow the previously delineated series of electrophysiological and molecular characteristics, tend to be horizontally-oriented basket cells that contact somata. LTS cells, instead, are vertically-oriented bipolar or bitufted cells that form synapses with dendrites. Not only do these two cell populations function in complementary directions, but their sites of contact onto other cells differ as well. For instance, FS cells, which synapse onto somata, impact the local generation of sodium-dependent action potentials; while LTS cells, which synapse onto dendrites, modulate generation of both sodium-dependent and calcium dependent action potentials (McBain and Fisahn 2001; Miles and Poncer 1993). It could be said then that LTS cells are more modulatory, while FS offer a more strengthened degree of

inhibition, as has been demonstrated experimentally: IPSCs recorded in pyramidal cells are typically larger when produced by FS interneurons than they are if produced by LTS (Xiang et al. 2002). Projection onto other inhibitory interneurons occurs as well: paired chemical connections exist between LTS cells and FS cells, and to a lesser degree, between dual LTS cells (Gibson et al. 1999). An interneuron can also self-synapse and thereby modulate its own activity. FS cell GABAergic autaptic transmission is in large part responsible for its precise, rapid, and non-adapting action potential progression fired in response to an injected depolarizing pulse (Bacci and Huguenard 2006). While LTS cells do not self-inhibit in this same way, they have been demonstrated to modulate self-activity in a more long-term capacity via the production of autocrine endocannabinoids (Bacci et al. 2004).

Interneurons also receive input from excitatory principal neurons and inhibitory GABAergic interneurons (Kawaguchi and Kubota 1993; Markram et al. 2004; Somogyi et al. 1998). Excitation of inhibitory neurons occurs to either produce feed-forward inhibition or to complete a feedback loop, as has been demonstrated electrophysiologically. EPSCs recorded from interneurons are faster than the corresponding events in pyramidal cells (Buhl et al. 1997; Geiger et al. 1997; Hestrin 1993), indicating that these cells receive this information first and therefore may interfere in some way with pyramidal cell reactivity. Some interesting differences exist between FS and LTS cell types in regard to their received excitatory inputs. FS cells are preferentially innervated by thalamocortical afferents (Gibson et al. 1999), while LTS tend to receive more synapses from a single pyramidal cell (Buhl et al. 1997). Reyes et al. demonstrated that somatic (and perisomatic) domain-targeting interneurons respond to excitatory inputs with paired-pulse depression, while those that target dendrites respond with paired-pulse facilitation (Reyes et al. 1998). More specifically, somatic-targeting PV-immunoreactive multipolar cells

(FS) demonstrate a depressive response, while dendrite-targeting bitufted SS-immunoreactive cells (LTS) demonstrate facilitated eEPSCs (Reyes et al. 1998). These opposing responses can simultaneously be observed from different PV or SS interneurons innervated by the same pyramidal cell (Reyes et al. 1998; Wang et al. 2002). Further, one interneuron innervated and stimulated by multiple pyramidal cells will produce the same distinguishing response, regardless of each pyramidal cell's differing time course (Markram et al. 1998).

1.5.4 Microgyral effect on LTS and FS-expressing interneurons and hypothesis

Until this point, discussion has comprised several cortical components that upon alteration, yield a hyperexcitable, epileptogenic cortex. Previous work has determined that there is increased functional excitatory input to the PMR and resultant hyperexcitability; and that from this hyperexcitable area, epileptiform activity can later be evoked (Jacobs et al. 1999a). Interneurons, and the alterations they undergo in malformed cortex, may play a role in this demonstrated delay in epileptogenicity, as well as in the generation of the epileptiform activity itself.

By the second postnatal week in lesioned rats, interneurons may enable unchecked excitation to dismantle the E/I balance. Secondly, the interneurons themselves undergo subtype-specific alterations that could encourage epileptogenesis within the PMR; these changes do not disrupt the identity of these cells (Buckmaster and Dudek 1997; Dinocourt et al. 2003). Rosen et al., has demonstrated a selective, infragranular decrease of PV-immunostaining interneurons (Rosen et al. 1998). That is to say, PV-immunostaining, known to correspond with FS cells, is shown to be decreased in cortical layers V and VI. Concurrently, at P14-15, there does not appear to be a change in SS-immunostaining interneurons within PMR (Patrick et al. 2006). Such

a reduction in presumed FS cell density and therefore, activity, would greatly lessen horizontally-rectified inhibition. Since overall functional inhibition is unchanged, this suggests that where horizontal intralaminar FS inhibition is weakened, other forms of inhibition might increase to compensate. Such compensation might take the form of a relative strengthening of vertical intracolumnar inhibitory component put forth by LTS cells (Figure 1.1). One potential consequence of strong intracolumnar inhibition may be increased synchrony (Bush and Sejnowski 1996). Without the horizontal component to inhibit spread into neighboring columns, the strong LTS-induced synchronous activity could propagate rapidly and without impedance, thereby promoting epileptiform activity. In support of this, previous studies in Jacobs' lab (not yet published) demonstrate that LTS cells in PMR cortex have three times the excitatory input than their counterparts in control cortex. Additionally, group 1 metabotropic glutamate receptors (mGluR₁ and mGluR₅), which selectively excite LTS interneurons, and not FS, display increased excitation in PMR, as well as anomalous activity and western blot expression of mGluR₅, not seen in control.

Therein lies the general hypothesis of this study: LTS interneurons are more active and therefore have more modulatory influence over excitatory cortical activity in PMR cortex, than in control cortex. Experiments in this work will assess the role of LTS interneurons with optogenetics.

1.6 Optogenetics

1.6.1 History and modern applications

Relatively recent in its accessibility as a neuroscientific technique, optogenetics has come to fulfill a technical need previously worked around. Before its inception, the ability to

manipulate individual components of the brain at a high temporal and spatial resolution was not reasonably achievable. Electrical, genetic, and pharmacological manipulations, while technically indispensable, lack such precision (Fenno et al. 2011). Francis Crick foresaw the need for tools like optogenetics in 1999 when he suggested that assembling heavy neuroscientific concepts, such as theory of mind, would require methodology “by which all neurons of just one type could be inactivated, leaving the others more or less unaltered” (Crick 1999; Fenno et al. 2011). Optogenetics fulfills precisely this requisite, allocating a way for researchers to specifically target “neurons of one type” and selectively “inactivate” them, while monitoring others in a functioning circuit (Wilson et al. 2012), as Crick so shrewdly predicted not so long ago.

Optogenetics is the functional combination of optic and genetic technologies that make it possible to image or control specific targets within living and intact neural circuitry (Deisseroth et al. 2006). Principally, transgenic technology is used to delineate specific neuronal targets, while light is used to control precise, simultaneous activity of the specific cell population, leaving nearby neurons of other type to presumably function as they would ordinarily (Deisseroth et al. 2006). Using this technique, researchers can acquire long-term *in vivo* imaging of labeled cells as well as simultaneously image functional, long-range brain maps with dynamics of neuronal morphology (dendritic spine growth and etc., Deisseroth et al. 2006; Petreanu et al. 2007; Wang et al. 2014). Dissection of neural networks is also possible: being able to directly observe a neuronal subtype’s contribution to overall circuitry and *in vivo* brain function at this level of spatiotemporal specificity was not previously possible. For example, Kvitsiani et al. was able to determine the relationship between PV and SS-expressing interneuron subtypes as it pertains to regulation of information flow during behavior in a particular pre-frontal cortical circuit; it was revealed that a select subtype of SS cells respond preferentially

when reward is introduced, while others expressing PV respond at reward leaving (Kvitsiani et al. 2013). Additionally, researchers can biochemically and electrically control genetically targeted neurons within intact living neural circuits (Deisseroth et al. 2006). This can take the form of behavior manipulation (Nagel et al. 2005; Yizhar et al. 2011), cortical rhythmicity modulation (Cardin et al. 2009), sleep induction (Tsunematsu et al. 2011), as well as control of specific neuronal populations to induce a therapeutic effect (Lin et al. 2014).

1.6.2 Genetically targeted optical control of neurons

The specific and direct targeting of neurons, as is central to optogenetics, is a result of genetic modification. Cells of a specific type can be modified to contain certain light-sensitive opsin molecules, or rhodopsins. These transmembrane proteins are encoded by single genes and take many forms. Depending on the type, they may induce varying effects among the cells upon which they reside (Fenno et al. 2011). The work in this correspondence involved the use of two membranous rhodopsin proteins, both encoded by type I microbial opsin genes (Fenno et al. 2011). The first of which, channelrhodopsin, is a cation-selective channel. Upon absorption of blue light (450-490nm wavelength), this channel will conduct monovalent and divalent cations, causing depolarization (excitation) in neurons upon which it is expressed (Nagel et al. 2003; Fenno et al. 2011). The second type to be discussed in this work, archaerhodopsin, is a more recently discovered outward proton pump that hyperpolarizes (silences) neurons upon absorption of yellow-green light (~575nm wavelength, Tsunematsu et al. 2013; Chow et al. 2010). These optogenetic actuators operate in a single-component format. That is to say, they combine tasks of light sensation and ion flux into a single protein unit (Fenno et al. 2011). This is noteworthy, especially when comparing the advent of these rhodopsin molecules with earlier multi-

component techniques, which were inherently more expensive and difficult to replicate between labs (Deisseroth et al. 2006). Ultimately, these single-component channels allow a way to noninvasively study the contribution of neurons with high cell-type resolution, using light.

There are many ways to incorporate rhodopsin channels into neurons. In this series of studies, Cre-Lox recombination was implemented. Cre-Lox is a site-specific recombination tool commonly used to target an intended DNA modification to a specific cell type. In this case, it was used to integrate or knock-in channelrhodopsin or archaerhodopsin into LTS interneurons, using Somatostatin (SS) as the promoter. The system involves a single enzyme, Cre recombinase, which recombines *Lox* sequences, or short targets for the purpose of carrying out insertions, deletions, and more (Madisen et al. 2012). Fundamentally, mice strained with Somatostatin-Cre Recombinase were bred with mice possessing *Lox* sequences containing the gene for both the intended channel and a reporter (green fluorescent protein, GFP). The result is Cre-Lox mice with either channelrhodopsin or archaerhodopsin, plus reporter, inserted at the original SS site (Madisen et al. 2012).

In conjunction with the freeze-lesion animal model for induced microgyria, knock-in of these channels to SS-containing cells, which correspond with LTS interneurons, will provide a way to selectively target these cells, manipulate them, and demonstrate biologically whether or not they exert a more powerful influence in PMR cortex. Interneurons have been studied in similar fashion for many years; the following section will provide a condensed survey of previous hallmark interneuron-focused optogenetic studies.

1.6.3 Study of interneurons using optogenetics; potential problems to consider

In recent years the investigation of interneurons using optogenetics has steadily moved to the forefront of neuroscientific research. Work done using this technique has revealed even more information about interneuronal functioning, tied as inextricably to their identities as their determined morphologies, intrinsic capabilities, and molecular patterns. Here, select works involving the aforementioned interneuron types outlined in the preceding section, VIP, PV (FS), and SS (LTS), will be discussed.

Cortical interneurons expressing vasoactive intestinal peptide (VIP) are now known to engage in disinhibition (Pi et al. 2013). Work in a 2013 study performed by the Kepecs group, combined optogenetics with single-cell recording techniques to determine the functional role of these interneurons and their underlying circuitries in differing parts of cortex. VIP interneurons were targeted by use of a VIP-Cre mouse line to knock-in Channelrhodopsin-2 (ChR2) or by viral delivery (another method for rhodopsin induction, not discussed in this work). This novel series of experiments demonstrated for the first time *in vivo* that VIP interneurons functionally inhibit other interneurons, thereby relieving some of the inhibition on pyramidal cells; a concept otherwise known as disinhibition. How they contribute mechanistically to their cortical circuit was revealed with further *in vitro* studies; VIP interneurons were shown to monosynaptically inhibit other interneurons far more than pyramidal neurons (Pi et al. 2013).

Interneurons expressing PV have also been a target of interest for many groups. In 2005, the duo Kuhlman and Huang explored the viability of Cre knock-in mice by targeting PV-expressing FS interneurons with ChR2; this group revealed not only the robustness of using Cre recombinase as a means to incorporate rhodopsins in a cell-type specific and long-term manner, but also the capacity for PV inhibitory circuits to re-wire in post-adolescent cortex via *in vivo*

imaging of PV interneuron axonal structure dynamics as visualized by axonal bouton dynamism (Kuhlman and Huang 2008). Another group in 2012 transfected both ChR2 and Arch (Arch) into cortical PV cells to demonstrate, via bidirectional manipulation, their functional contribution within *in vivo* visual cortex. Apparently, PV interneurons within visual cortex have tight control on the cortical response to visual stimuli for all contrasts and orientations, particularly due to its post-synaptic contribution to layer II/III pyramidal cells (Atallah et al. 2012). Optogenetics combined with electrophysiological (whole-cell) recordings in another work within the striatum revealed that PV interneurons (ChR2 expression induced by viral injection) provide feedforward inhibition directly and indirectly to major striatal projection neurons (Szydlowski et al. 2013). Since striatal and neocortical circuits both characteristically comprise a major projecting neuronal population interconnected with a small yet diverse population of interneurons, studying the circuitry of PV in both areas is vastly applicable; in fact, the PV targeting pattern observed in the striatum is similar to that seen from PV cells onto pyramidal cells of neocortex (Szydlowski et al. 2013). Finally, Cardin et al. tested a popular hypothesis regarding PV interneuron's functional contribution to the induction of cortical gamma oscillations via optogenetic manipulation of these cells *in vivo*. It was predicted that these oscillations are generated by synchronous activity of PV-expressing FS interneurons. With the use of ChR2, the group was able to observe a causal relationship between gamma oscillation and PV cells for the first time (Cardin et al. 2009). In these studies, excitatory cells were also virally infected with ChR using CAMKII as the promoter, demonstrating another cell type that can be studied with optogenetics.

SS-expressing interneurons are a third popular target. A study in 2013 identified SS cells to play a novel role in layer IV of barrel cortex microcircuitry: apparently, SS interneurons

within this particular layer, target PV interneurons primarily (as opposed their traditional targets, pyramidal neurons), resulting in disinhibition. Inhibiting SS neurons in this study, using layer IV-specific transfection of Halorhodopsin onto SS cells (another type of inhibitory rhodopsin not discussed in this correspondence), caused an increase in PV firing, and consequent decrease in the firing of pyramidal cells, paramount to a disinhibitory pathway (Xu et al. 2013). Not only did this study reveal a new neocortical function of SS interneurons, but it also demonstrated that it is possible to have rhodopsin expression also be layer specific (Xu et al. 2013). Adesnik et al in another novel circuit dissection study, this time within the visual cortex, identified SS interneurons to first of all be preferentially excited by horizontal cortical axons, and secondly to contribute to surround suppression; a phenomenon previously unknown to have a contribution by a cortical circuit. Work in this study also involved layer-specific expression of ChR2 for selective excitation and either Arch or Halorhodopsin for selective inhibition (Adesnik et al. 2012). Another group, Wilson et al, transfected with ChR2, SS-expressing and PV-expressing interneurons together to optically dissect the effects of distinct interneuron classes within a functioning network. Using a custom built two-photon imaging system, combined with optogenetic stimulation, this group was able to image responses at a temporal resolution. Complemented with recordings from non-infected neurons in slices of visual cortex, this group demonstrated that dendrite-targeting SS interneurons subtract more information from excitatory cells and thereby sharpen selectivity, while soma-targeting PV interneurons divide responses, and preserve selectivity (Wilson et al. 2012). Royer et al completed a dual SS and PV study similar to this within the hippocampus and using inhibitory Halorhodopsin. They determined certain specific characteristics (rate, timing, and burst firing) of pyramidal cell activity that are controlled directly by these two interneuron types (Royer et al. 2012).

The technologies previously discussed are exciting, innovative, and obviously inspiring, causing many research groups to publish many significant findings. However, there are some issues with this rush, mainly regarding the expression patterns of certain Cre-mouse lines. The (LTS) SS-Cre mouse line, for instance, used in many high-profile studies, has a 6-10% chance of expression in PV-expressing cells (Hu et al. 2013). Co-expression is a factor neglected by many studies, but one to bear in mind, particularly given the pursued high cell-type resolution principal to optogenetics.

As inspired by many of the studies listed above, work in this communication will utilize ChR and Arch to selectively study the altered contribution of SS-immunostaining LTS interneurons within PMR, as it pertains to the induction of epileptiform activity.

1.6.4 Optogenetics and epilepsy

There are many instances of optogenetics being used to research epilepsy. One study performed in 2013 discussed the ability to induce seizure-like afterdischarges with repetitive photostimulation *in vivo*. ChR2 was expressed (virally) throughout the hippocampus; repeated instances of blue light shone onto this area was sufficient to induce these events, which became self-sustained and propagated throughout the hippocampus (Osawa et al. 2013).

Complementarily, another study of the same year demonstrated the amelioration of severe epileptic seizure onset *in vivo*. The group silenced Halorhodopsin-expressing hippocampal pyramidal neurons with light and thereby demonstrated the essential role they play in seizure-induction within the hippocampus (Sukhotinsky et al. 2013). Lastly, Ledri et al expressed ChR2 in a mixed population of interneurons to determine their collective impact on ongoing epileptiform activity in *ex vivo* (acute) hippocampal slices. When SS and PV interneurons were

simultaneously excited with blue light, epileptiform activity was suppressed. Suppression occurred to a far lesser degree if only one of the two interneuron subtypes was activated individually (Ledri et al. 2014).

It is clear that optogenetics is a robust technique, with many broad applications; from the dissection of networks to the manipulation of cortical rhythmicity, this tool can be applied as well to the study of interneurons and how they contribute to intractable epilepsy as induced by microgyria. In the following series of experiments, optogenetics, along with whole cell recordings, field potential studies, and immunohistochemistry, was utilized to investigate cortical SS (LTS) interneurons within layer V of somatosensory cortex, as they pertain and potentially contribute to the induction of epilepsy in an animal model for polymicrogyria.

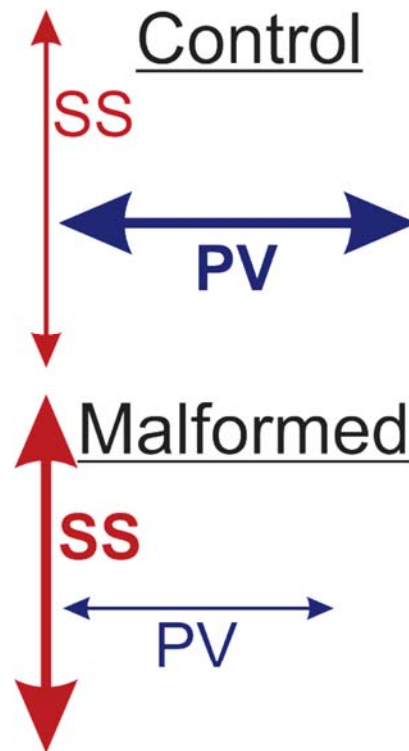


Figure 1.1 Graphic representation of PV and SS inhibition as they differ between control and PMR cortex. In control cortex, the horizontal, intralaminar inhibition by PV interneurons stronger than SS interneuron vertical, intracolumnar inhibition. In malformed cortex, within PMR, it is believed that this is switched: higher SS interneuron inhibition and lessened FS inhibition potentially contributes to the pathological genesis of epileptiform activity within PMR.

Chapter 2

The Effects of Optogenetic Activation and Silencing of SS interneurons within Malformed, Epileptogenic Cortex

2.1: Hypothesis and objectives

Polymicrogyria, a developmental cortical malformation, can cause intractable epileptic seizures in afflicted individuals. This debilitating disorder and lack of effective therapeutic intervention drives a need to elucidate the underlying cellular mechanisms inherent to cortical malformations of this nature.

These studies utilize a freeze-lesion model for polymicrogyria in transgenic mice that selectively express either Channelrhodopsin or Archaelhodopsin optogenetic channels on one particular cell type implicated by previous studies, SS-immunostaining LTS interneurons. These cells, within an epileptogenic area adjacent to the malformation proper, termed the paramicrogyral region (PMR), are thought to be functionally altered, as compared to their state in homologous control cortex, and potentially contribute to the pathological generation of epileptiform activity within malformed cortex.

We hypothesize that SS-immunostaining, LTS interneurons have greater modulatory control over excitatory neurons within pathological PMR. With the following series of experiments, we assessed this by:

1. Evaluating if they elicit greater suppression of excitatory fields in PMR cortex via field potential studies
2. Evaluating if their imparted effect is larger in PMR cortex via whole cell patch clamping of pyramidal neurons

All recordings were taken from pyramidal neurons and LTS interneurons within layer V of somatosensory cortex PMR (500-600 μm away from the freeze-lesion induced microgyrus) or homologous control cortex.

2.2: Materials and Methods

Channelrhodopsin2 and Archaeorhodopsin3 induction into LTS interneurons

To achieve expression of light-sensitive Channelrhodopsin or Archaeorhodopsin in SS-expressing LTS interneurons, Ai32 (RCL-ChR2 (H134R)/EYFP) or Ai40 (RCL-Arch/EGFP)-D mice were bred with SS-IRES-Cre mice. The result was offspring that expressed either a Channelrhodopsin-2/EYFP (ChR2-EYFP) or Archaeorhodopsin-3/EGFP (ArchT-EGFP) fusion protein in SS-expressing cells, respectively.

Freeze lesion surgery

Aseptic surgery techniques were followed to induce bilateral freeze lesions in mice on postnatal day 1 (P1). SS-ChR2-EYFP or SS-ArchT-EGFP mouse pups were anesthetized via induced hypothermia achieved by being placed on ice for 4 minutes. A coronal incision was made on the scalp, exposing the skull. A freezing probe, comprising a copper bar with a 0.1 mm pointed tip cooled to -55°C was applied directly onto the skull approximately 0.5 mm lateral to midline sagittal suture and equidistant between the coronal and lambdoid sutures, on both sides, corresponding to somatosensory cortex (Figure 2.1). The probe was applied for a duration of five seconds. The skin was sutured, the pups were warmed over a heating blanket for 10 minutes, and returned to the dam. Animals were weighed for five days following the surgery to ensure proper recovery.

Brain extraction and acute slice preparation

Naïve control and lesioned animals aged either P12-21 were anesthetized with an overdose of isoflurane and decapitated. The brain was quickly removed and immediately transferred into freezing (-18°C) sucrose slicing solution containing (mM): 2.5 KCl, 1.25 NaH₂PO₄, 10 MgCl₂, 0.5 CaCl₂, 26 NaHCO₃, 234 sucrose, 11 glucose. Coronal slices containing somatosensory cortex were cut using a 1000 plus vibratome at a thickness of 300 µm; slicing occurred with the brain submerged in sucrose slicing solution. Somatosensory cortex was confirmed with corresponding hippocampal morphology (Figure 2.1). Slices were transferred and stored in a holding chamber in artificial cerebrospinal fluid (aCSF) infused with 95% O₂/5% CO₂ to maintain pH; aCSF comprised (mM): 126 NaCl, 3.5 KCl, 1.25 NaH₂PO₄, 1.0 MgSO₄, 1.2 CaCl₂, 10 glucose, and 26 NaHCO₃. Slices remained in this solution heated to 34°C for 25 minutes, followed by a 20-25 minute cooling period and thereafter at room temperature until recording.

Electrophysiology and optical manipulation

Prior to recording, slices were transferred from the holding chamber to the recording chamber with aCSF (~300 mOsm) infused with 95% O₂/5% CO₂ and heated to 32°C flowing over for entire duration of experimentation. In some instances, aCSF bath solution was modified to contain gabazine (GABA_A receptor antagonist, 20 µM), or APV (NMDA antagonist, 50 µM) & DNQX (AMPA antagonist, 20 µM).

Intracellular solutions for pyramidal cell and LTS interneuron recordings were either of a 'high chloride' configuration (in mM: 70 K-gluconate, 10 HEPES, 4.0 EGTA, 70 KCl, 4.0 Na-

ATP, and 0.2 Na-GTP) or a 'regular' configuration (in mM: 130 K-gluconate, 10 HEPES, 11 EGTA, 2 MgCl₂, and 2.0 CaCl₂, 4.0 ATP, and 0.2 GTP). Osmolarities and pH of both intracellular solutions were adjusted to 280-290 mOsm and pH 7.3. Biocytin or Alexa-495 (0.25-0.5%) was included in recording pipettes to confirm neuronal morphology post-experiment via subsequent staining.

In some patch clamp experiments an electrical stimulus was applied 100-150 μ m lateral to patched cell using a glass pipette filled with either aCSF or 1 M NaCl. For field potentials, the recording electrode was pulled in the same manner as a whole cell patch pipette (~1-2 μ m diameter) and filled with aCSF or 1 M NaCl. In order to activate and record a field potential, a stimulating electrode (the same as used in patch experiments, described above) was placed in layer V, vertically beneath a field potential recording electrode in layer II/III. These recordings were made using a Multiclamp 700B amplifier (Molecular Devices) and digitized at 50 kHz with Digidata 1440A and pClamp software (Molecular Devices).

Optical manipulation of LTS interneurons was achieved using X-Cite and XLED1 software (Lumen Dynamics). To activate ChR expressing SS neurons, a wavelength of 460 nm was used at an intensity of either 20% (SS interneuron recordings, LED evoked pyramidal neuron IPSCs, electrically-evoked pyramidal neuron IPSCs) or 100% (horizontal and vertical shift LED evoked pyramidal neuron IPSCs). To activate Arch-expressing SS neurons, a wavelength of 565 nm was used, all at an intensity of 100%. These wavelengths were applied through a 60X objective either above patched cell, or at varying distances depending on the experimental protocol. Applied light covered an area of ~100 μ m as determined by the objective's aperture diameter.

Some additional field potential recordings not requiring optical activation were made on a separate rig, where slices were placed in an interface chamber and recordings were made using an ER1 amplifier (Cygnus Technologies), and digitized at 5-10 kHz with pClamp software and a Digidata 1322A (Molecular Devices).

The utilized experimental protocols were as follows: (1) an LED stimulation intensity series wherein 11 increasing durations of LED, ranging from 0.1 to 2 milliseconds, were applied in three series. This series was applied with LED exposure over the layer V patched cell, 200 μm lateral, 400 μm lateral, or in superficial layers II/III. (2) A repetitive stimulation series wherein five flashes of blue LED, at the duration threshold for the patched pyramidal neuron, was applied at a frequency of 50Hz; exposure in this case was above the layer V patched pyramidal neuron. Repetitive stimulation was applied in three series. (3) LED was also applied over the patched pyramidal neuron during a six second collection of spontaneous events split into a two second pre-light period, a 2 second during-light period, and a 2 second post-light period, repeated for a series of six sequences. (4) An electrical stimulation intensity series, wherein electrical stimulation, starting at the millivoltage that evoked an all-or-none threshold response, was applied at 1, 2, 4, 8, and 16 times the threshold amount, from a distance of 100-150 μm to the layer V patched pyramidal neuron; intensities were applied in three series. (5) An electrical stimulation plus LED combination series, wherein the same electric stimulation intensity series described above was applied with a simultaneous LED component that occurred during the electrical stimulation, and continued for 20 milliseconds following cessation of the electrical component; combination intensities were applied in three series. (6) Field potential recordings comprising electrical stimulation intensity series, as described above, however with stimulation in layer V, and the recording element vertically above in layers II/III. Threshold in these

experiments was a current level that evoked a short latency negative field of 0.2 mV amplitude response. (7) Field potential recordings with series electrical stimulation as described above plus a simultaneous LED component both applied in layer V, with the recording element vertically above in layers II/III. LED application occurred during electrical stimulation and continued for 20 milliseconds following cessation of the electrical component.

Tissue Staining

Experimental slices were placed in 4% paraformaldehyde for 24 hours after experimentation was completed. After this period, slices were placed into phosphate buffered saline (PBS) until staining. Whole cell patch clamp slices with biocytin-filled cells were stained with either combination NeuN (mouse anti-NeuN conjugated with Alexa Fluor 488, Chemicon MAB377X) and avidin (1:500 Texas Red conjugate, Life Technologies) or avidin alone. Images of slices reacted with avidin were imaged using the Leica TCS-SP2 AOBS confocal laser scanning microscope in VCU's department of Anatomy and Neurobiology microscopy facility. Images of slices reacted with Neun were obtained with the Scope A1 microscope (Zeiss) and Image Pro Premiere 9.1 (Media Cybernetics).

Data Analysis

Data was analyzed using Clampfit (Axon Instruments), Minianalysis (Synaptosoft), and home-written macros in Microsoft Excel. Data are presented as mean \pm SEM. In most cases, a 2-way repeated measures ANOVA was performed (SPSS software from IBM, significance set at $p < 0.05$), for instance to compare across various stimulus intensities in control versus PMR.

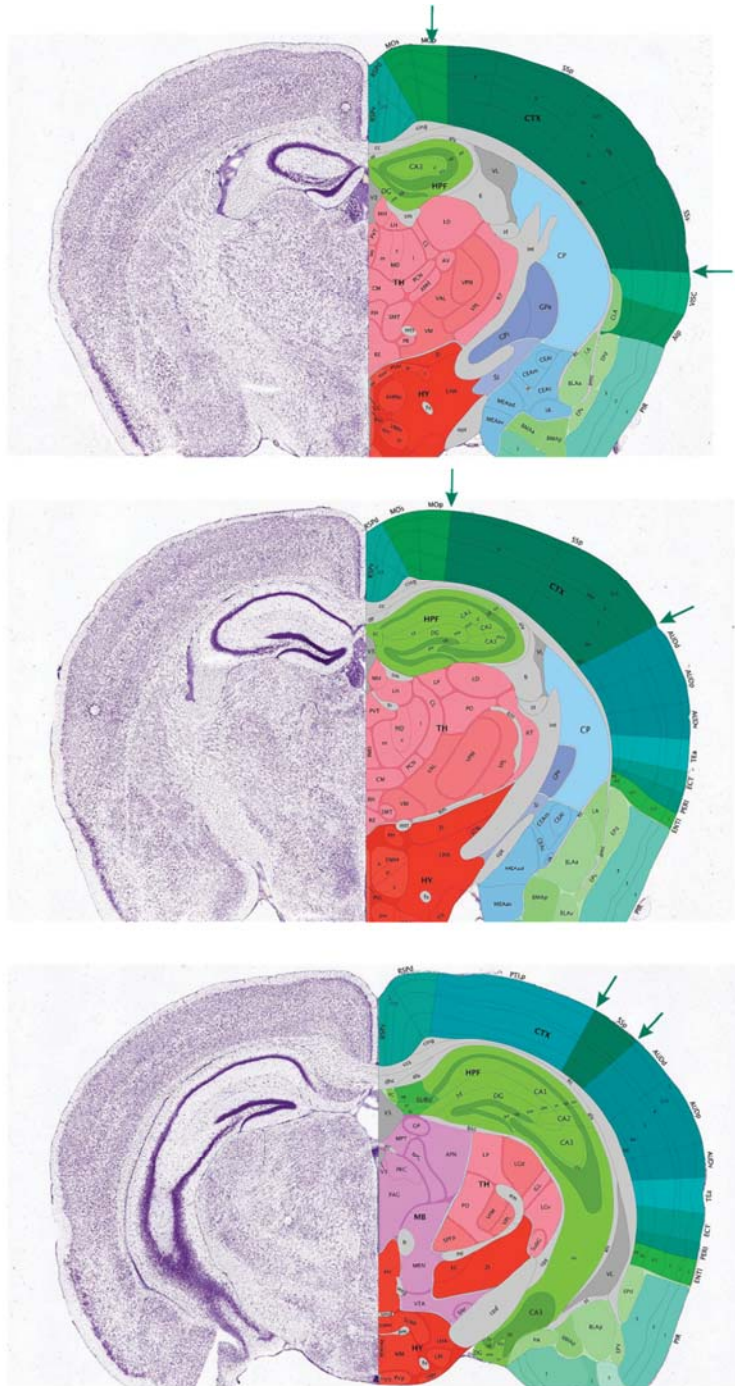


Figure 2.1 Figures from the Allen Brain atlas. Primary Somatosensory Cortex is shown in dark green (arrows).

Lein, E.S. et al. (2007) Genome-wide atlas of gene expression in the adult mouse brain, *Nature* 445: 168-176. doi: 10.1038/nature05453. Website: © 2015 Allen Institute for Brain Science. Allen Mouse Brain Atlas [Internet]. Available from: <http://mouse.brain-map.org>.

Bottom image: <http://atlas.brain-map.org/atlas?atlas=1&plate=100960232#atlas=1&plate=100960081&resolution=8.38&x=5728&y=3696&zoom=-3>

Chapter 3

Results

3.1 Freeze lesion at P1 in mouse produces similar histopathology to that observed in the P1 rat

These studies are the first in this lab to utilize the freeze-lesion methodology in mice—previous studies implemented the surgery technique in rats. Thus, our first goal was to demonstrate that the histopathology and functional hyperexcitability could be replicated in this species. Slices prepared and used for electrophysiological recordings were immersion fixed for 24 hours, subsequently placed in PBS, and later stained for NeuN. These slices showed a visible sulcus and abnormally laminated region (microgyrus) in somatosensory cortex, as it developed from the induced P1 freeze-lesion. Two examples are provided, to be compared with an imaged section of homotopic control cortex (Figure 3.1A, B, and C). Note that identification of the region as somatosensory cortex can be made by comparing to sections from a published atlas (Figure 2.1), using the location relative to the midline, as well as the morphology of hippocampal structure as guides.

Higher power images revealed variability of microgyral lamination patterns between slices (previously described, Figure 3.1E and F). Such variability is also typical of microgyri produced in rats (Jacobs et al. 1999a). Finally, the transition from microgyric layers 1-4 to normal layers I-VI was visualized (Figure 3.1F).

All whole cell patch clamp recordings were made within layer V cortex, mid-PMR (500-600 μm lateral to microgyrus) or in homotopic control cortex, as visualized by red hashed-line boxes in Figure 3.1 A, B, and C (PMR begins 0.5 μm away from the microgyrus, and continues

for $\sim 1.5 \mu\text{m}$). All field potential recordings were made in layer II/III vertical to a stimulating component in layer V within the same range.

3.2 Freeze lesion in P1 mouse produces epileptiform activity within PMR

To ensure that the model expresses functional hyperexcitability in mice as it does in rats, electrically-evoked field potentials were recorded in slices taken from control and PMR mice aged P12 to P18. From PMR slices, instances of interictal-like (Figure 3.2D) and ictal-like (Figure 3.2E) epileptiform activity was evoked. Occasionally, instances of subtle epileptiform activity was evoked in control slices (Figure 3.2B), but this is attributed to the developmental age of the mice and has previously been demonstrated in rats as well (Luhmann et al. 1998). Ictal-like epileptiform activity was never evoked in control slices. Of the total animals tested, epileptiform activity was evoked in 100% of PMR-containing mice (Figure 3.2F). However, epileptiform activity was not evoked from some slices within this group.

3.3 SS interneuron activation effect on evoked field potentials

Selective activation or silencing of SS/LTS interneurons is made possible by the specific expression of ChR2 or Arch on SS-containing cells respectively, enabling us to manipulate these cells in predictable ways, so as to observe the effects they might have in their networks.

Effect of SS-ChR2 interneuron activation on field potentials

To assess the effect selective SS-ChR2 interneuron activation has on a field potential, electrically-evoked field potential responses were recorded and then compared to responses recorded with the same electrical stimulus protocol but the addition of blue (b)LED applied

(described above). Application of bLED would stimulate SS interneurons, causing them to fire and inhibit postsynaptic neurons; in these experiments, an increase in inhibition would be expected to produce a suppression of the short latency field potential negativity. Example electrical and electrical plus bLED recordings from single control (Figure 3.3A) and PMR slices (Figure 3.3B) are shown. Single slice examples of electrical plus bLED fields can be seen as they compare to electrical only (Figure 3.3C). The degree of bLED effect between these two slices appears to be less in the PMR slice as indicated by percent of remaining electrically-evoked response following bLED suppression (Figure 3.3D). Statistical analyses were not performed since this series comprised 1 control slice and 1 PMR slice.

3.4 Pyramidal cell and SS/LTS interneuron identification and differentiation

Neuronal morphology

Subsequent experimentation involved recordings from either pyramidal neurons or SS/LTS interneurons within layer V PMR or homotopic control cortex. These types were identified in several ways. One way was morphologically as visualized in the live slice under DIC optics. Morphology was confirmed by post-hoc avidin staining of slices with biocytin-filled cells (Figure 3.4 A, B, C, and D). Additional methods of identification including intrinsic firing patterns will be discussed in subsequent sections.

In the example pyramidal cell shown in Figure 3.4, morphological characteristics typical of pyramidal neurons are seen. These include the presence of a large and triangular soma with a large diameter apical dendrite projecting towards pia, basal dendrites below the soma and the presence of a long axon that projects subcortically (Figure 3.4A). Morphological confirmation of SS/LTS interneurons involved the same process. These cells can be seen to differ from

pyramidal neurons in a few ways: they lack an apical dendrite and typically possess a thin axon projecting towards pia as shown in Figure 3.4B. A higher powered image of the same cell shows the ovular soma, multipolar pattern of dendrites, and a thin pia-oriented axon (Figure 3.4D), all characteristics typical of LTS interneurons.

Intrinsic firing patterns

Electrophysiologically, cell types can be determined by the pattern of action potentials fired in response to intracellular injection of depolarizing current. We employed this as our third way to identify and differentiate between cell types. One identifying characteristic in a series of action potentials evoked in this way is the size of the first action potential's afterhyperpolarization period (AHP) in relation to that associated with the last action potential (Gibson et al. 1999). Injection of depolarizing current into the pyramidal cell shown in Figure 3.4A and C yielded a series of action potentials, the first of which had an AHP smaller in amplitude (more depolarized) than that of the final AHP (top, Figure 3.4E). Injection of the depolarizing current into the SS/LTS interneuron shown in Figure 3.4B and D evoked a series of action potentials where the first AHP was larger in amplitude (more hyperpolarized) than the last (bottom, Figure 3.4F). These patterns correspond with pyramidal cell and SS interneuron firing patterns, respectively (Gibson et al. 1999). To differentiate these neurons from FS interneurons, action potential duration and adaptation was reviewed. FS interneurons, as their name suggests, have a fast action potential, typically less than one millisecond in duration. In addition, they show little to no adaptation even at high firing frequencies. In the example pyramidal and SS/LTS neurons, it can be seen that the action potential duration is much longer than one millisecond (Figure 3.4E and F).

3.5 The effect of SS-ChR2 activation in pyramidal neurons

SS-ChR2 interneuron responsiveness to bLED

A series of control experiments were performed to confirm that ChR2 opsin channels operate similarly in control and PMR cortex. Ultimately, these studies were performed to verify that channel functioning was not altered by induced microgyria inherent to the utilized animal model. Results in this section are from whole cell patch clamp recordings of SS interneurons identified prior to patching with cellular fluorescence. Selective fluorescence is possible because of the SS-expressed opsin's GFP or YFP reporter protein.

SS interneurons expressing ChR2 responded (depolarized and fired action potentials) to bLED (20% intensity) similarly in control and PMR animals for the durations of light used here. In current clamp (bath solution: regular aCSF; regular intracellular solution), action potentials were recorded as induced by a bLED stimulation intensity series (described above). In most cases, cells responded to all durations of 0.2 milliseconds and higher with one to three action potentials (Figure 3.5). Shown in Figure 3.5 are examples of these recordings from single control and PMR SS interneurons, demonstrating the most typically seen response pattern: most commonly, a cell would fire one action potential at the lowest durations (0.1 and 0.2 milliseconds) and increase firing to between two and three action potentials at the highest duration (two milliseconds). This pattern was demonstrated in both control and PMR SS interneurons. The mean number of bLED-evoked action potentials at all durations was similar between these two groups as determined by a two-way repeated measures analysis of variance (Figure 3.5C): there was no statistically significant effect of group (control versus PMR), $F(1,14) = 0.005$, $p = 0.944$; or any significant interactions between group and bLED duration, $F(10,140) = 0.657$, $p = 0.480$. There was, however a significant effect of bLED duration, $F(10,140) =$

9.145, $p = 0.003$), indicating simply the responses evoked by shorter bLED durations were not the same as ones evoked by longer bLED durations.

Unless otherwise noted, most reported statistics to follow were also generated by two or three-way repeated measures analyses of variance and will be presented using the preceding format.

bLED-induced pyramidal cell IPSCs

To test the hypothesis that SS interneurons have more modulatory control over excitatory principle (pyramidal) neurons within layer V PMR, we assessed the effect selective activation of SS interneurons has. These results are from layer V pyramidal neuron whole cell patch clamp recordings.

SS-ChR2 interneurons, as described above, are activated (depolarized) by bLED. Their activation will inhibit the neurons they presynaptically contact. Inhibition can be visualized electrophysiologically in voltage clamp as inhibitory postsynaptic currents (IPSCs), allocating a way to measure the effect selective activation of SS interneurons has on pyramidal cells. In active cortex and within the same postsynaptic cell, IPSCs will occur with the simultaneous induction of excitatory postsynaptic currents (EPSCs), as induced by excitatory neurons. To isolate the inhibitory component, excitatory glutamatergic receptor blocking agents, APV and DNQX were added to bath aCSF; high Cl intracellular solution was used as well. These experiments comprised bLED stimulation intensity series (defined above) recorded in voltage clamp (holding = -70 mV). Shown in Figure 3.6 are examples of select intensities recorded in a single control and PMR neuron. IPSC peak amplitudes evoked by bLED durations of 0.5 milliseconds and higher, in PMR pyramidal neurons, were more than double than that of control

pyramidal neurons (Figures 3.6A and B) and thusly, the peak amplitude of IPSCs were much larger in PMR pyramidal neurons compared to those from control pyramidal neurons (Figure 3.6C): there were statistically significant effects of group, $F(1,10) = 12.020$, $p = 0.010$; bLED duration, $F(10,100) = 24.240$, $p = 0.000$; and significant interactions between bLED duration and group, $F(10,100) = 8.680$, $p = 0.000$. The area of significant IPSC peak response was also larger in PMR pyramidal neurons (Figure 3.6D). In this measure, there was a statistically significant effect of bLED duration, $F(10,100) = 5.640$, $p = 0.000$.

Changes in the neurotransmitter release probability of presynaptic SS interneurons is a likely contributor to the demonstrated increase in PMR pyramidal neuron inhibitory response. If PMR SS interneurons have a higher release probability than those in control, then the postsynaptic neuron will respond to repeated evocations with a higher degree of attenuating IPSCs due to a higher likelihood of neurotransmitter depletion each time. Lower presynaptic release probability would have the opposite postsynaptic effect. To test this in SS-ChR2 interneurons, we employed a repetitive stimulation series (described above, voltage clamp; holding = -70 mV). EPSC blockers in bath were used to isolate the inhibitory component (high Cl^- intracellular solution used as well). Repetitive LED stimulation of SS interneurons at 50Hz demonstrated a relatively higher release probability in PMR pyramidal neurons. Both control (Figure 3.7A) and PMR pyramidal neurons (Figure 3.7B) showed depression in their respective SS interneuron-evoked sequence of IPSCs, however, the depressive response was greater in PMR pyramidal neurons, indicating a relatively higher probability of release in presynaptic PMR SS interneurons (Figure 3.7B, C). The percent of peak one for peaks 2-5 was compared between control and PMR using a 2-way ANOVA. This revealed a significant effect of condition (each

peak compared to peak one), $F(3,54) = 46.220$, $p = 0.000$; but no significant effect of group (control vs PMR), $F(3,54) = 1.410$, $p = 0.250$.

To determine the distance from which pyramidal neurons can respond to bLED activation of SS-ChR2 interneurons, IPSCs from LED stimulation intensity series (described above; EPSC blockers in bath, high Cl intracellular solution) were recorded with bLED application over the area of the original patched layer V pyramidal neuron (frame 0). This was compared to the same evoked by bLED applied at distances of 200 μm (frame 2) and 400 μm (frame 4) lateral to the patched pyramidal cell. IPSCs evoked with bLED over the layer V patched cell were also compared with those evoked by bLED applied in superficial layers II/III, vertical to layer V cell position (voltage clamp; holding = -70 mV).

Single cell examples qualitatively show that IPSC peak lessens when bLED stimulus is applied at farther distances (Figure 3.8A and B). There were statistically significant effects of bLED location, $F(2,10) = 9.255$, $p = 0.027$; and bLED duration, $F(10,50) = 14.738$, $p = 0.001$, on IPSC peak amplitude between control neurons (Figure 3.8C, 3.9A). Between PMR neuron IPSC peak amplitudes, there was a statistically significant effect of bLED duration, $F(10,30) = 8.739$, $p = 0.044$; and significant interactions between location of bLED and bLED duration, $F(20,60) = 6.786$, $p = 0.041$ (Figure 3.8D, 3.9A). Specifically, between frame 0 and frame 2 IPSC peak amplitudes in PMR pyramidal neurons, there was a statistically significant effect of bLED duration, $F(10,30) = 8.663$, $p = 0.000$; significant effect of bLED location, $F(1,3) = 34.084$, $p = 0.010$; and a significant interaction of bLED duration and bLED location, $F(10,30) = 4.649$, $p = 0.000$. Between frame 0 and frame 4 IPSC peak amplitudes, there was a statistically significant effect of LED duration, $F(10,30) = 19.152$, $p = 0.000$; and significant interactions between bLED duration and bLED location, $F(10,30) = 17.616$, $p = 0.000$. There was no significant effect of

bLED location, $F(1,3) = 7.519$, $p = 0.071$. (Figure 3.9D). In figure 3.9B, control and PMR bLED-evoked IPSCs at frame 2 and frame 4 are graphed as a percentages of IPSCs evoked in pyramidal neurons at frame 0; there are no significant effects of bLED duration, $F(1.331,10.645) = .989$, $p = 0.369$; bLED location, $F(1,8) = 1.329$, $p = 0.282$; group (control versus PMR), $F(1,8) = 0.585$, $p = 0.466$; nor are there any significant interactions (statistical reports omitted as all p -values > 0.05).

Pyramidal neuron IPSC peak amplitudes of LED at frame 0 (layer V) were also compared to the same of bLED application in superficial layers II/III (vertically above patched pyramidal cell). IPSC peak amplitudes were different between these two stimulation sites as there are statistically significant effects of bLED duration $F(1.776,7.103) = 15$, $p = 0.003$, bLED location $F(1,4) = 8.773$, $p = 0.041$, and significant interactions between group (control and PMR) and bLED duration, $F(3.891,15.565) = 4.264$, $p = 0.017$ (Figure 3.10A, 3.10B). The occupied percentage of frame 0 IPSC peak amplitude shows that control and PMR pyramidal neurons show a similar decrease in response to bLED application in layers II/III: there is no statistical significant effect of group (control versus PMR) in this measure, $F(1,4) = 4.672$, $p = 0.097$. This indicates that whatever differences do exist between the functional input by SS interneurons in layer V versus layer II/III, between control and PMR, are restricted to layer V.

bLED effect on evoked pyramidal cell events

To further assess SS-Chr2 interneurons as they might be altered in PMR cortex, we added an electrical component to evaluate the effect their selective activation imparts on electrically-evoked events. These results are from whole cell patch clamp recordings taken from pyramidal neurons stimulated by an electrode placed at a lateral distance of 100-150 μm to the recorded

neuron (electrode within pipette filled with either regular aCSF or 1M NaCl; voltage clamp, holding = -70 mV). Electrically-evoked IPSCs (APV and DNQX in bath, high Cl intracellular solution) were evaluated to be compared with the electrically-evoked plus simultaneous bLED application (protocols described above).

Electrical stimulation in this way will evoke an inhibitory postsynaptic current from the patched pyramidal neuron. Since the addition of SS interneuron-stimulating bLED will further activate SS interneurons within this area, electrical plus bLED pyramidal neuron responses should therefore be smaller than those evoked by electrical stimulation alone.

In control pyramidal neurons, there were no statistically significant effects of condition (electrical stimulation versus electrical plus LED), $F(4,8)=1.504$, $p = 0.288$; or significant effects of stimulation intensity, $F(1,2) = 0.017$, $p = 0.909$ (Figure 3.11A). In PMR pyramidal neurons, there were no significant effects of condition (electrical stimulation versus electrical plus LED), $F(1,3) = 1.582$, $p = 0.297$; or significant effects of stimulation intensity, $F(4,12) = 0.863$, $p = 0.513$ (Figure 3.11B); however we believe that upon the addition of more cells to the group, these data may become significant. By calculating the percent change of electrical plus bLED IPSCs from electrical-alone, we can see that there was no change in controls, but in PMR, responses were reduced to about 50% (Figure 3.11 E). Again, with our currently small sample size of 3 control and 4 PMR pyramidal neurons, there is not currently a significant difference between these two groups in this measure (Figure 3.11D): there was no statistically significant effect of group (control and PMR), $F(1,5)=1.601$, $p = 0.262$; and no significant interactions between group (control and PMR) and electrical stimulus intensity, $F(4,20) = 1.985$, $p = 0.203$.

3.6 The effect of SS-Arch silencing in pyramidal neurons

SS-Arch interneuron responsiveness to yLED

A series of control experiments were performed to confirm that Arch opsin channels operate similarly in control and PMR cortex. Just like with SS-ChR2, these studies were performed to verify that channel functioning was not altered in the utilized animal model. Results in this section are also from whole cell patch clamp recordings of SS/LTS interneurons identified prior to patching with selective reporter-protein fluorescence.

SS interneurons expressing Arch respond (hyperpolarize) to yellow light (yLED; 565 nm, 100% intensity). yLED stimulation intensity series (defined above) were recorded in SS interneurons in current and voltage clamp (bath solution: aCSF containing 50 μ M APV & 20 μ M DNQX; high Cl intracellular solution). These series evoked hyperpolarization events similarly in control and PMR SS interneurons. Responsiveness was not as robust as it was in SS-ChR2 interneurons, however, the longest LED durations in the series did evoke hyperpolarization (Figure 3.12). We note here that we applied the yLED for two milliseconds, a duration shorter than what is required for the channels to fully open (five milliseconds); thus these experiments need to be repeated with longer yLED exposures. Current clamp (CC) hyperpolarizing events occur downwards (Figure 3.12A), while those recorded in voltage clamp (VC) occur upwards (Figure 3.12B).

yLED effect on spontaneous events

The final parameter employed to assess the differing effect SS interneurons have in layer V PMR pyramidal neurons involved the selective silencing of SS-Arch interneurons during recordings of spontaneous IPSCs (APV and DNQX in bath, high Cl intracellular solution; voltage clamp, holding = -70 mV). These experiments comprised a six second long period of

spontaneous event collection with an intermediate LED component (described above; single cell example, Figure 3.13A). Change in IPSC frequency was used as the metric in this series of experiments. Frequencies of prelight and during light IPSC events remained the same in all recorded cells in both control and PMR (t-tests used to compare pre to during separately for each group: $p > 0.05$ at each comparison; Figure 3.12 B, C). While this was initially unexpected, we believe that the yLED had little effect because overall excitability levels were low due to APV and DNQX in the bathing medium, which reduced overall network activity and therefore also likely reduced firing of SS neurons. Activating the arch will only have an effect that is observable in neurons postsynaptic to the SS if the SS neurons with the Arch were already firing action potentials. If they are silent then hyperpolarizing them further would not be observed by recordings unless made directly from the SS neurons.

3.7 Summarized effects selective activation or silencing of SS interneurons has in control versus PMR cortex

The performed experiments revealed much about the SS interneuron functionality in control versus PMR cortex. bLED activation of SS-ChR2 interneurons evoked higher inhibitory postsynaptic events in layer V PMR pyramidal neurons compared to that of control. This could potentially be due to the release probability of these interneurons within PMR which was also demonstrated to be higher relative to controls. The increased output from PMR SS neurons appears to be largely confined to layer V locally around the activated SS neurons. This is true since the bLED IPSC produced by stimulation at 200 and 400 μm lateral to the recorded neuron was not significantly different. In addition, the bLED IPSC evoked from superficial layers above the recorded layer V pyramidal neuron was also not significantly different between control and

PMR. Only with bLED stimulation in layer V could the differences between control and PMR be observed. SS-ChR2 interneuron effects on electrically-evoked IPSCs recorded in pyramidal neurons were interesting: we believe that the following may become significant with a larger n, but currently our data suggests not only that the electrically-evoked IPSCs within PMR pyramidal neurons may be larger than those evoked in control, but the electrical and bLED IPSCs may demonstrate a pattern wherein PMR pyramidal neuron IPSCs are reduced more by SS interneuron activation than they are in control. Finally, yLED exposure onto SS-Arch interneurons did not appear to alter the frequency of spontaneous inhibitory events recorded from control and PMR layer V pyramidal neurons under these experimental conditions.

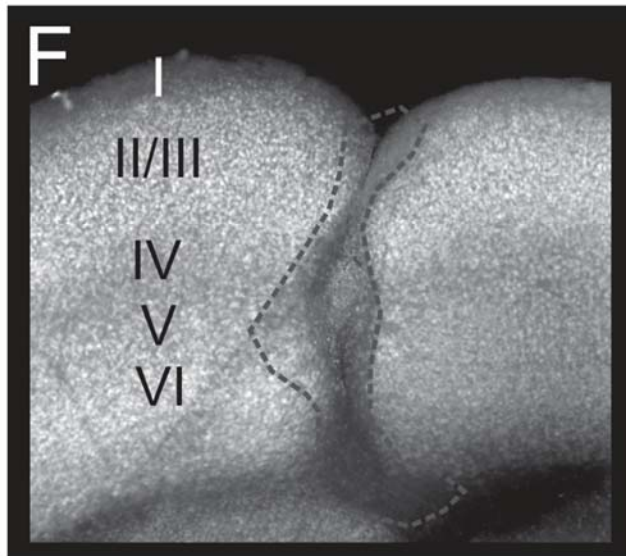
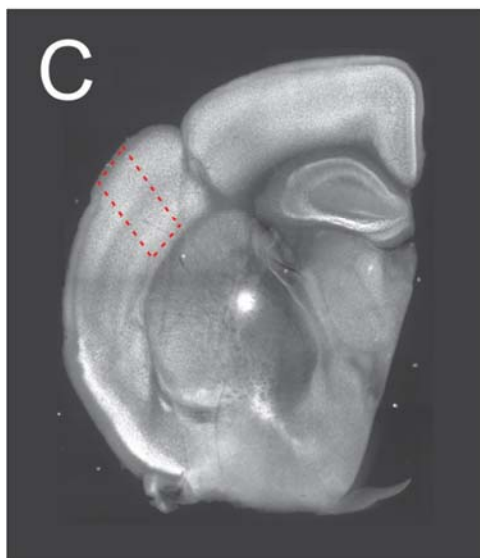
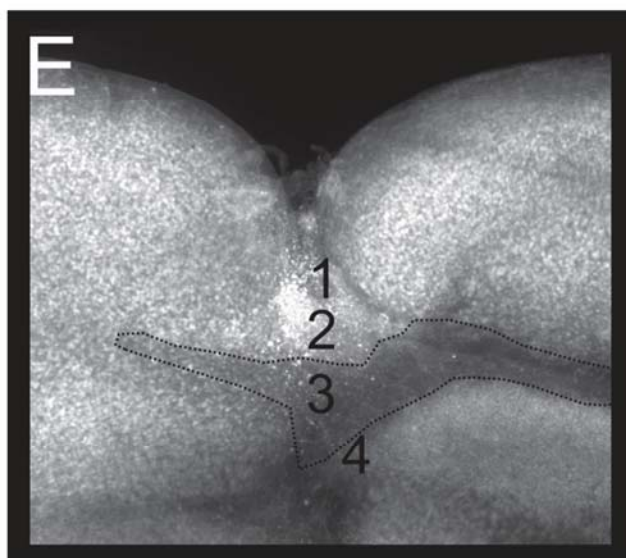
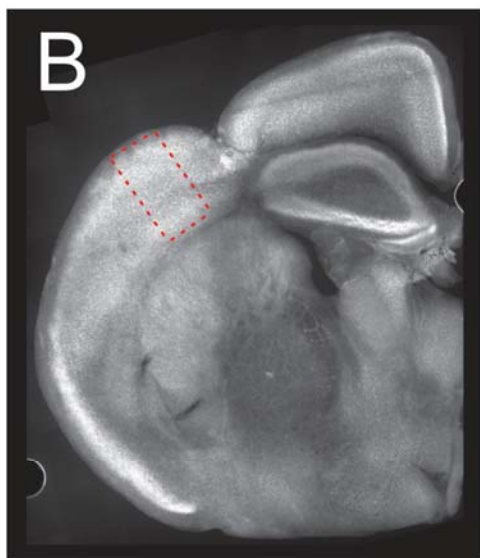
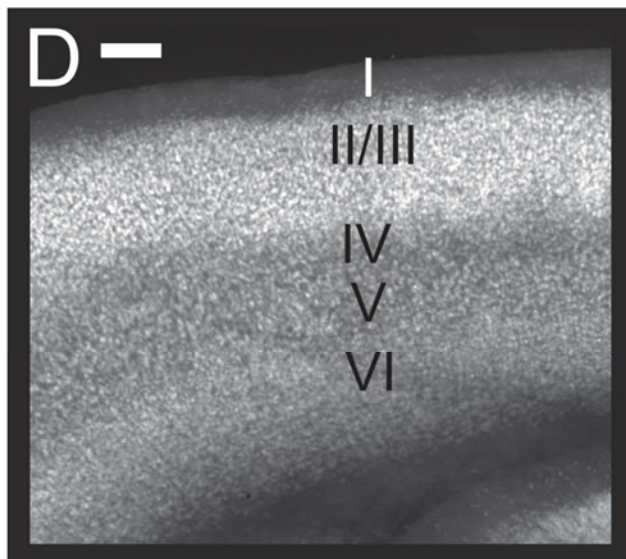
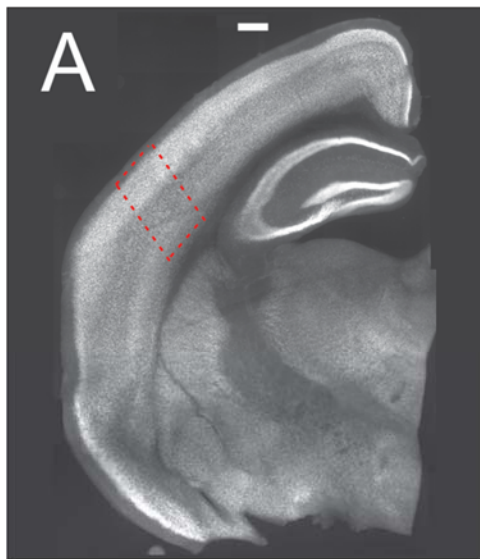


Figure 3.1 Examples of lamination pattern for control (**A**) and two examples of freeze-lesion induced microgyri (**B, C**) from mouse slices used for recordings. Dotted red boxes indicate the range within which all recordings were made. **D-F** higher power images of homotopic control cortex and two example microgyral regions taken from figures in **A-C**. Roman numerals indicate normal layers. Arabic numerals indicate microgyral layers as previously described. Dotted black line in **E** shows layer 3 of the microgyrus, which is a cell-sparse zone. Microgyral lamination pattern is harder to decipher in **F**, but this variability was typical even for the rat model. Dashed gray line shows malformed area. Adjacent transition to normal layers can be seen in **F**. Scale bar in **A** for **A-C** = 400 μm and in **D** for **D-F** = 200 μm .

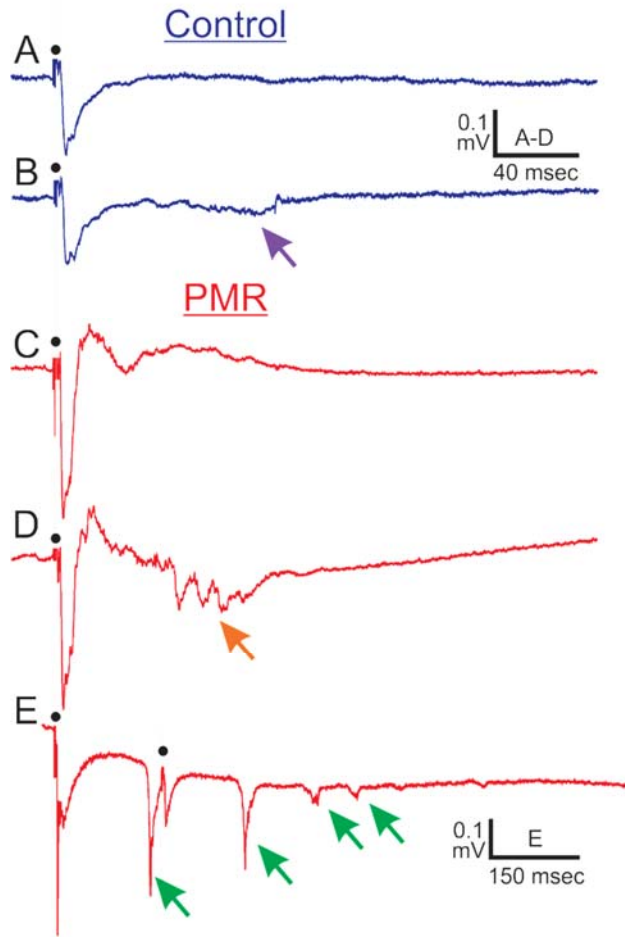


Figure 3.2. Field potential epileptiform activity electrically evoked in slices from P12-18 day old control (A, B) and freeze-lesioned (C, D, E) mice. A, C. Normal short latency field potential (stimulation at black dot). D. Interictal-like epileptiform activity (orange arrow) is evoked adjacent to the malformation. E. In some slices of malformed cortex ictal-like activity (green arrows) was evoked. Such activity was never seen in control cortex. F. Epileptiform activity was observed in 100% of 8 mice with malformed cortex (total of 18 slices). Similar to rats, at these developmental ages, some epileptiform activity was occasionally evoked in cortex from 9 control mice (19 slices). It was always more subtle (purple arrow in B) than any evoked in PMR cortex. * = z-test, $p < 0.05$, ** = $p < 0.01$.

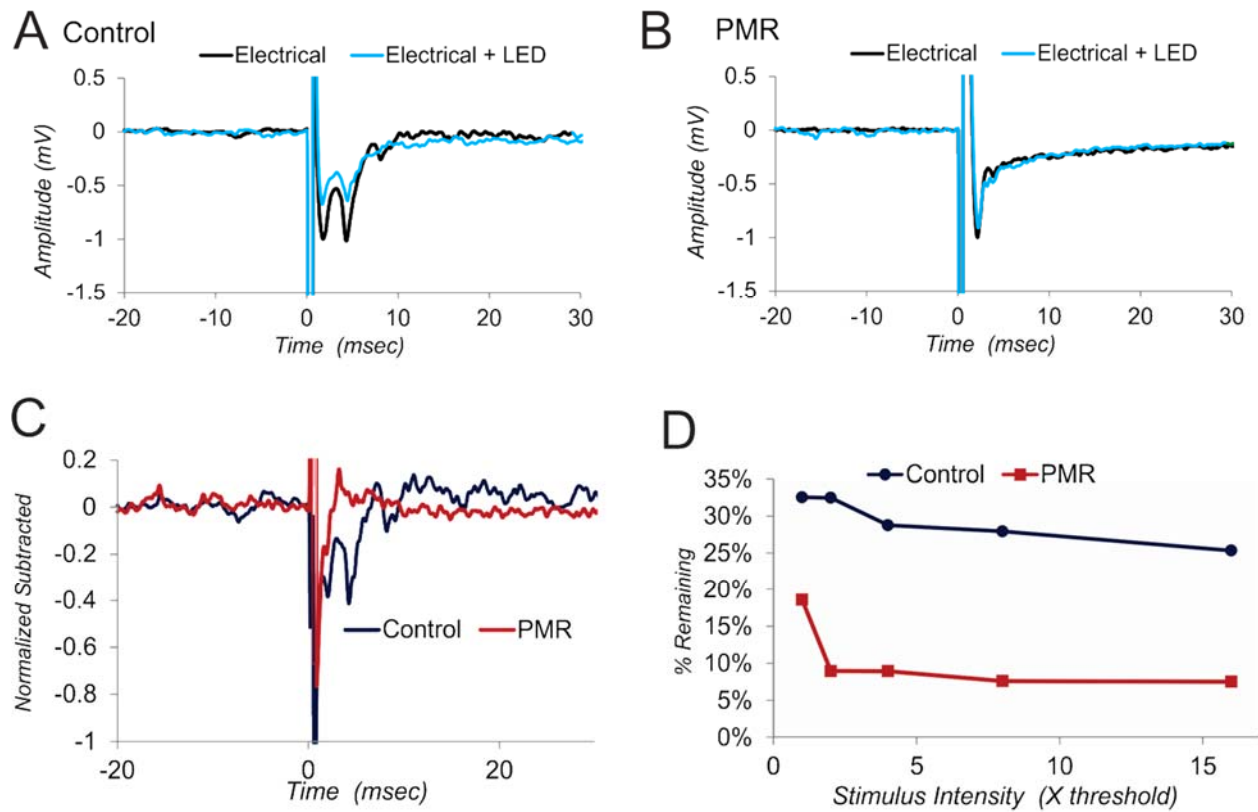


Figure 3.3 Electrical (black) and electrical + bLED (light blue) evoked field potentials recorded in control (**A**) and PMR (**B**) cortex containing ChR-SS neurons. These examples traces were normalized to the negative peak of the electrical only response. **C** Result of subtracting the two traces in A for control and in B for PMR (Electrical only - Electrical + bLED). **D** Percent of peak electrically evoked response remaining following subtraction of electrical + bLED from electrical only. Tissue from Cre-SS mice mated with floxed ChR mice. N= 1 control and 1 PMR.

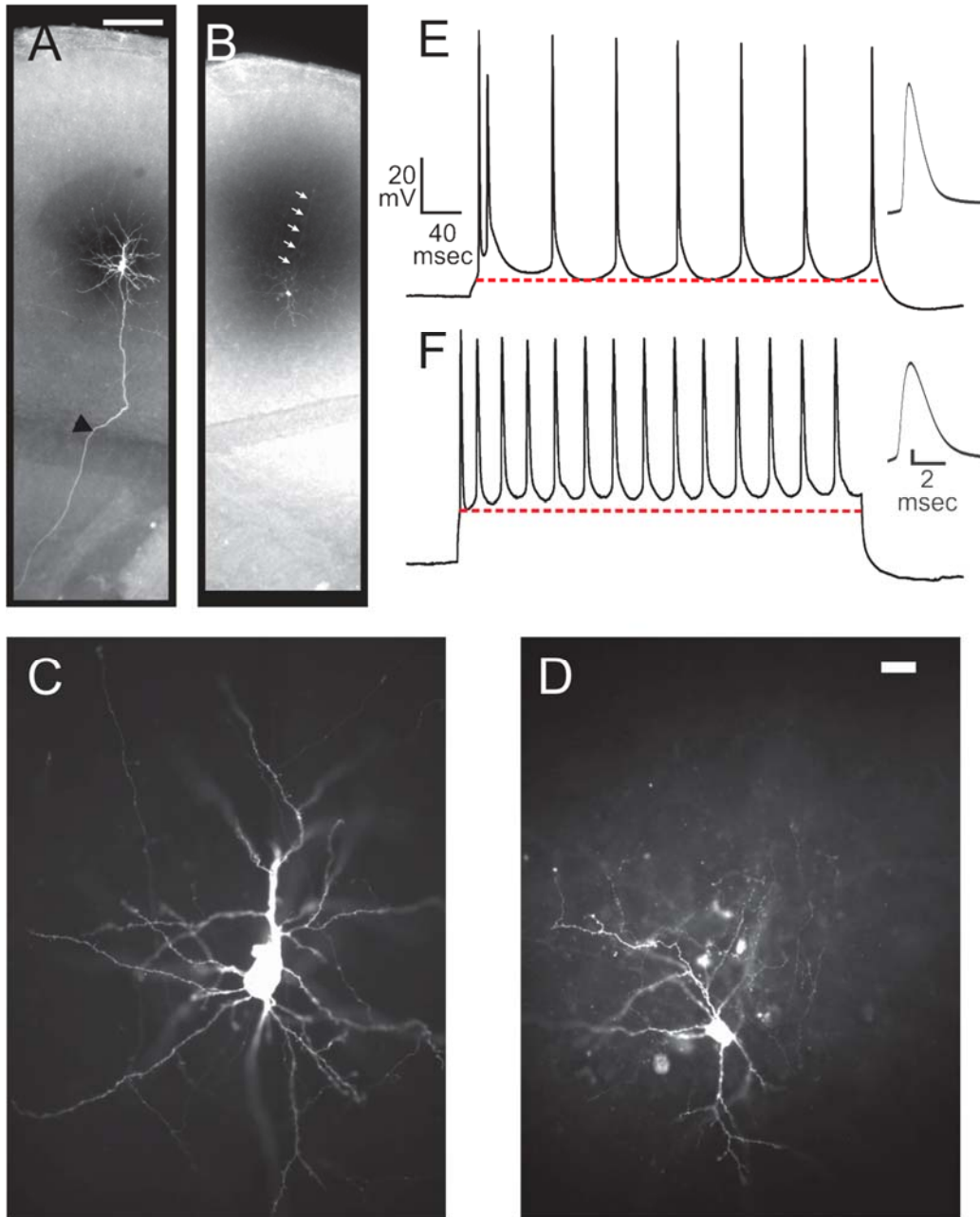


Figure 3.4 Two types of neurons from which whole cell patch clamp recordings were made for this study. **A)** Pyramidal neuron can be seen to have apical dendrite projecting towards pia and long axon that projects subcortically (black arrow). **B)** Interneuron lacks apical dendrite and has thin axon projecting towards pia. **C)** High power image of cell shown in A, triangular shaped soma can be seen with thick apical, as well as basal dendrites typical of pyramidal neurons. **D)** Interneuron is same as that shown in B, and is typical of somatostatin-containing low-threshold spiking neuron, has more oval shaped soma, with multipolar pattern of dendrites and thin axon. Scale bar shown in **A** is 200 μm for A and B, and in **D** is 20 μm for C and D. **E)** The action potential firing pattern produced by injection of depolarizing current into cell shown in A and C. This pattern is typical of a pyramidal neuron, since the last AHP is lower (more hyperpolarized) than the first AHP. **F)** The action potential firing pattern produced by injection of depolarizing current into cell shown in B and D. This pattern is typical of low threshold-spiking neurons, since the first AHP is lower than the last. Dark gray insets to the right of firing pattern show a single action potential (first in pattern to the left) expanded. An action potential duration longer than 1 msec distinguishes these cell types from fast-spiking interneurons. Scale bar is 10 mV and 2 msec for inset.

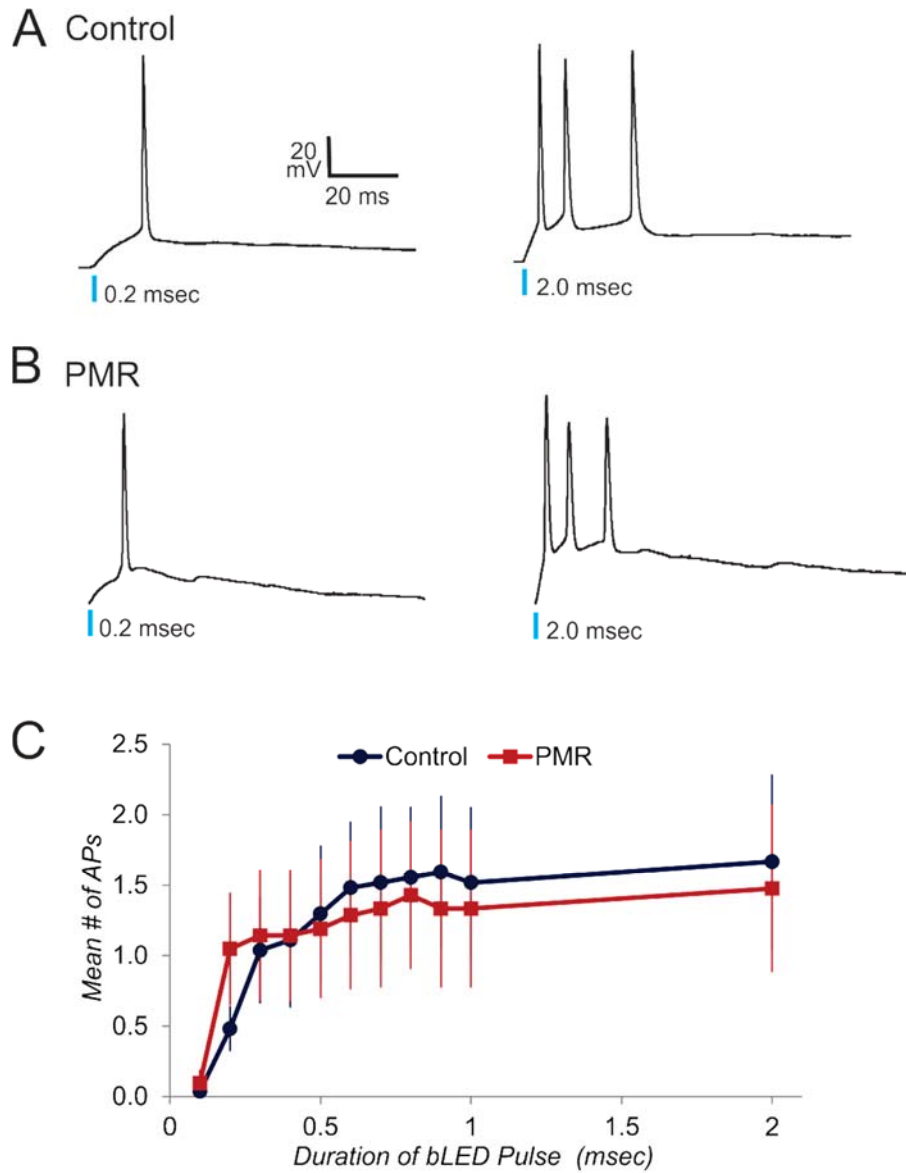


Figure 3.5 Result of bLED stimulation of control (**A**) and PMR (**B**) SS interneurons in tissue containing ChR-SS cells. **A, B** (left) Single action potential evoked by a 0.2 msec duration of bLED. **A, B** (right) Three action potentials evoked by a 2.0 msec duration of bLED. **C**. Mean number of action potentials evoked by bLED of increasing durations. These values are not different (unpaired t-test, $p > 0.05$). $N = 9$ control and 7 PMR SS identified with fluorescence prior to recording and with the electrophysiological signature of LTS neurons during recording.

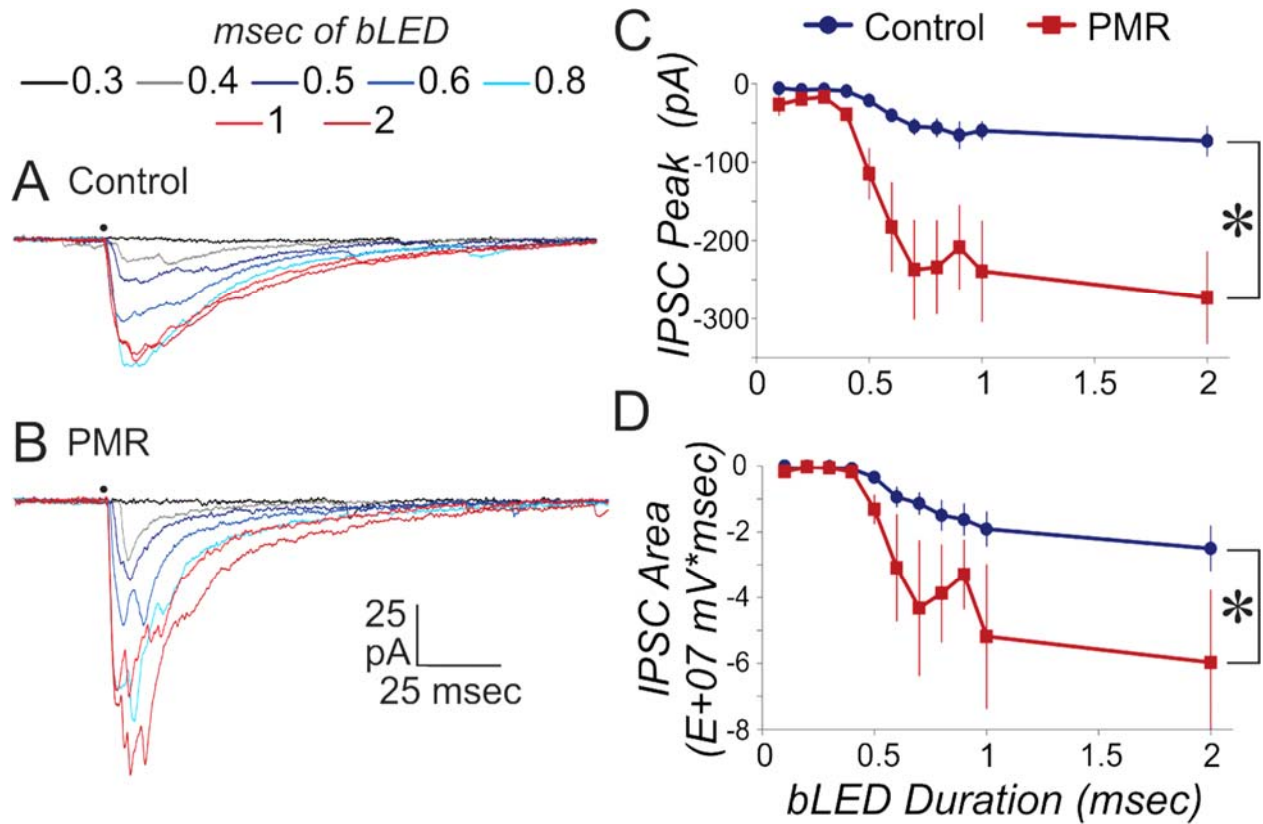


Figure 3.6 A, B. IPSC responses of control (A) and PMR (B) pyramidal neurons to bLED stimulation of varying durations in tissue containing ChR-SS neurons. Example traces are averages of 3 stimulus presentations from one neuron. **C, D.** bLED-evoked IPSC peak amplitude versus stimulus intensity (varied by increasing light duration). Graphs in C and D show Mean \pm SEM from 7 control and 5 PMR cells. 2-way repeated measures ANOVA indicate that data in both graphs are significantly different ($p < 0.05$)

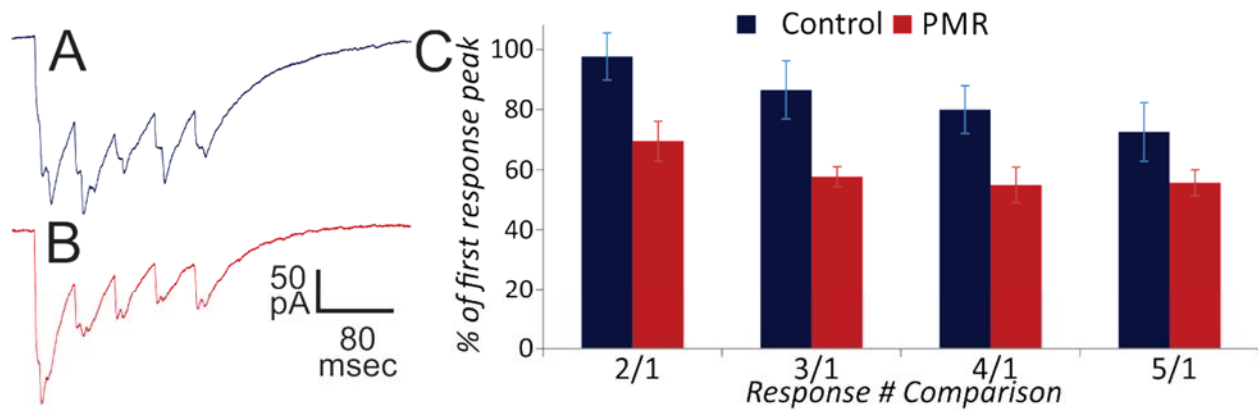


Figure 3.7 (Left) Relative probability of release can be estimated with repetitive stimulation. Here bLED was repetitively applied (for a duration of 2 msec) at a rate of 50 Hz in tissue containing ChR-SS neurons. Recordings were made in layer V pyramidal neurons. Example responses from a control (A) and a PMR (B) neuron (average of 5 stimulus presentations). C Summarized data: The peak IPSC amplitude for responses 2-5 was normalized to the peak of the first IPSC. IPSCs recorded in control neurons show a slightly depressing response. In PMR neurons the degree of short term depression in these IPSCs is greater compared to controls (2-way repeated measures ANOVA). This indicates an increased probability of release (more secure synapse) from SS to layer V pyramidal neurons in PMR cortex. Mean \pm SEM from 7 control and 5 PMR cells.

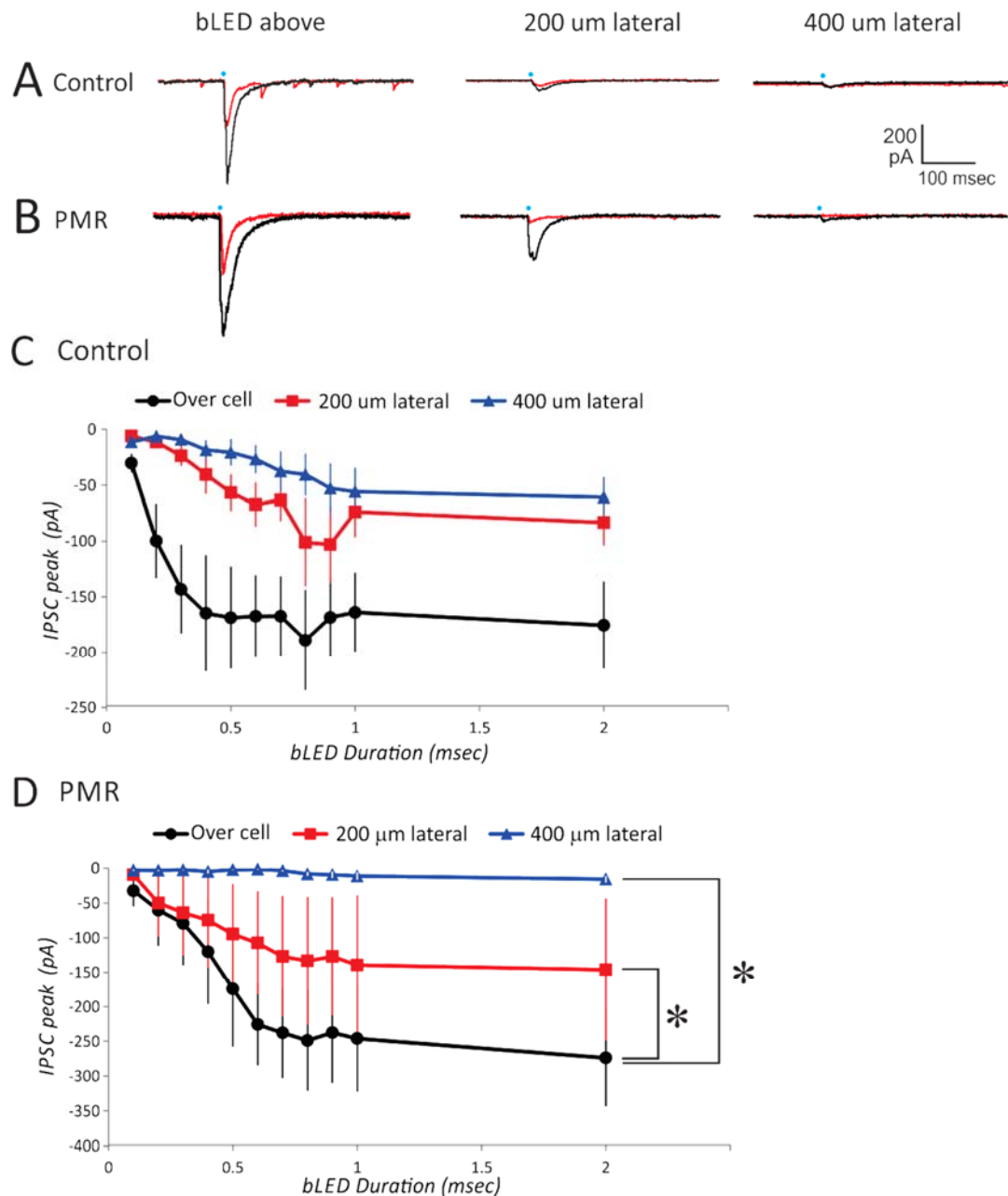


Figure 3.8 Comparison of bLED activation of SS neurons at different distances from the recorded neuron in tissue containing ChR-SS cells. Inhibitory synaptic currents were recorded in control (**A, C**) and PMR (**B, D**) layer V pyramidal neurons. The bLED was applied through the with LED objective at 3 locations from the recorded neuron: Frame 0 (F0), 0 (directly above), Frame 2 (F2), 200, and Frame 4 (F4), 400 mm lateral to the patched pyramidal cell. Examples from individual neurons for control (**A**) and PMR cortex (**B**) for 0.4 (red) and 1 msec (black) durations show qualitatively that IPSC peak lessens when bLED stimulus (blue dot) is applied at farther distances. **C, D.** Mean \pm SEM for peak IPSC versus bLED duration for 6 control and 4 PMR pyramidal neurons. A repeated measures ANOVA for control data shown in **C** suggests that there was a trend towards a decreased response with lateral difference ($p = 0.07$). For PMR data shown in **D** there was a significantly decreased response with lateral difference (2-way, repeated measures ANOVA, $p < 0.05$).

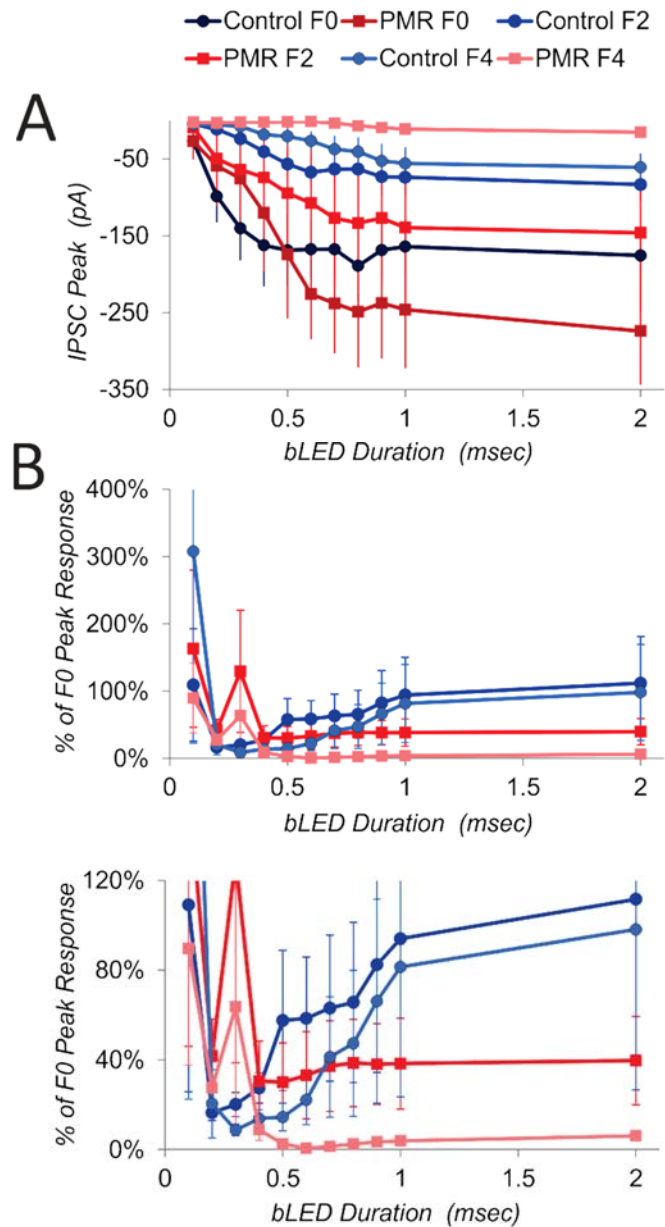


Figure 3.9 Recapitulation of data shown in Figure 3.8, bLED-evoked IPSCs recorded in pyramidal neurons in tissue containing ChR-SS neurons. Here the PMR and control values can be directly compared for 4 and 6 cells, respectively. **A.** A 2-way, repeated measures ANOVA showed a significant effect of bLED duration, and an effect of the interaction between subject group, stimulus intensity and condition. Further post hoc analysis of which conditions and bLED durations will show a difference between control and PMR after additional recordings are obtained.

B. The same control and PMR IPSCs recorded in response to bLED at F2 and F4, graphed as a percentage of IPSCs evoked in pyramidal cells after bLED at F0; bottom is a zoomed in portion of top for more detail of the comparison between control and PMR at long duration bLED intensities. A 2-way, repeated measures ANOVA showed no differences between control and PMR ($p > 0.05$).

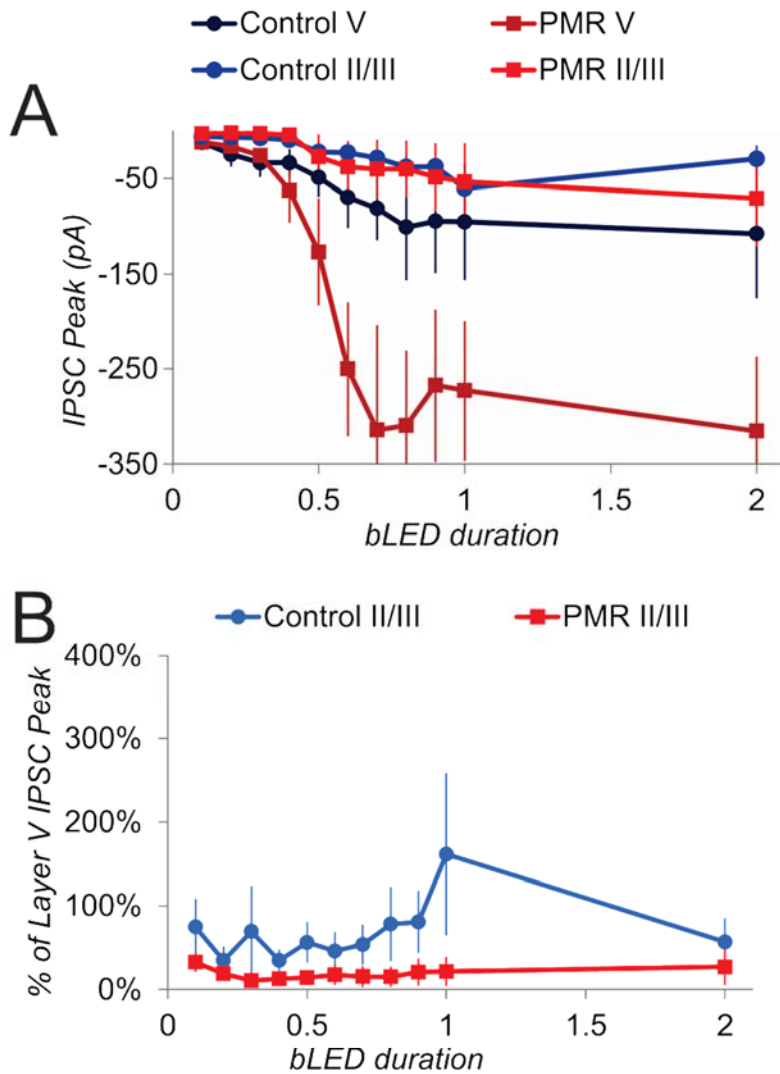


Figure 3.10 Comparison of bLED activation of SS neurons in layer II/III versus the F0 layer V responses recorded in tissue containing ChR-SS cells. These inhibitory synaptic currents were recorded from 3 control and 3 PMR layer V pyramidal neurons. For the Layer II/III activation, the 60X objective was moved to that layer directly vertical to the recorded neuron. **A.** Mean \pm SEM for the peak amplitude of the IPSC. A 2-way, repeated measures ANOVA showed a significant effect of location only ($p < 0.05$). **B.** The responses to bLED stimulation of layer II/III as a percent of the layer V (F0) response. Inhibitory synaptic currents recorded in control and PMR layer V pyramidal neurons, evoked by light activation of SS neurons with LED objective above the patched pyramidal cell in layer V, and in superficial layers II/III. For this data, a 2-way, repeated measures ANOVA showed an effect of intensity only ($p < 0.05$). Thus control and PMR show a similar decrease in the response to SS activation in layer II/III relative to that in layer V. An additional 2-way, repeated measures ANOVA was performed to compare IPSCs evoked by layer II/III stimulation in control versus PMR: ($p > 0.05$) the two groups are not different in this parameter.

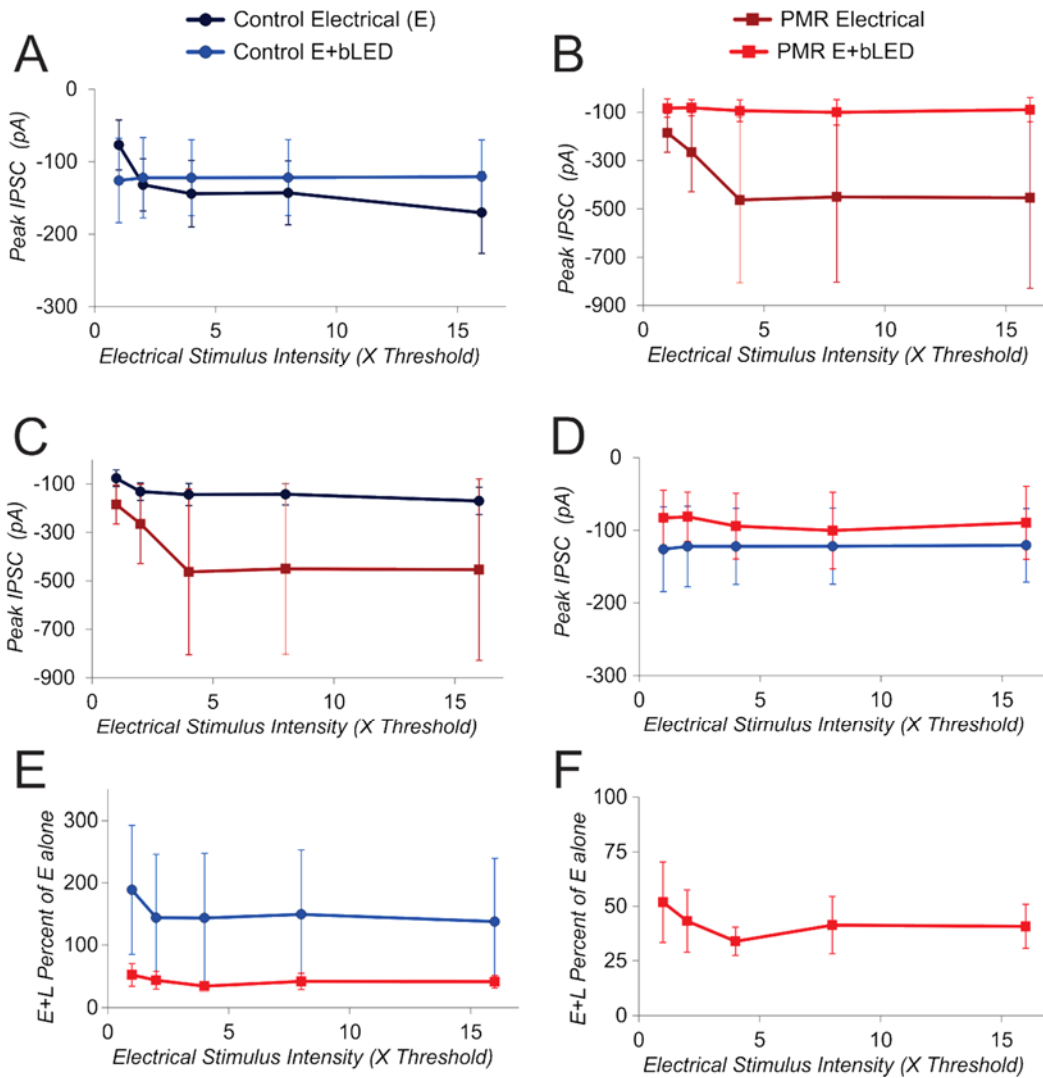


Figure 3.11 The effect of adding bLED-activation of SS neurons to the electrically-evoked IPSC recorded from pyramidal neurons in tissue containing ChR-SS neurons. In the ‘electrical + bLED’ condition, the bLED was turned on during the electrical stimulation and for 20 msec afterward. **A.** There is no effect of adding bLED in 3 control cells (2-way, repeated measures ANOVA, $p > 0.05$). **B.** In 4 PMR neurons, adding bLED trended towards causing a reduction in evoked-response (2-way repeated measures ANOVA, $p = .130$). **C.** Graph shows a direct comparison between the electrically-evoked IPSC in control vs PMR. **D.** Graph shows a direct comparison between the electrical + bLED stimulation in control vs PMR. **E, F.** The peak amplitude IPSC in response to electrical + bLED stimulation was divided by the peak response to electrical only. (Note that F is a rescaling of E). In control cells the responses are near or above 100%, while in PMR neurons the IPSC response is suppressed when bLED stimulation is added. This suggests that in PMR SS neurons may have a greater inhibitory effect onto other inhibitory interneurons than is true in control.

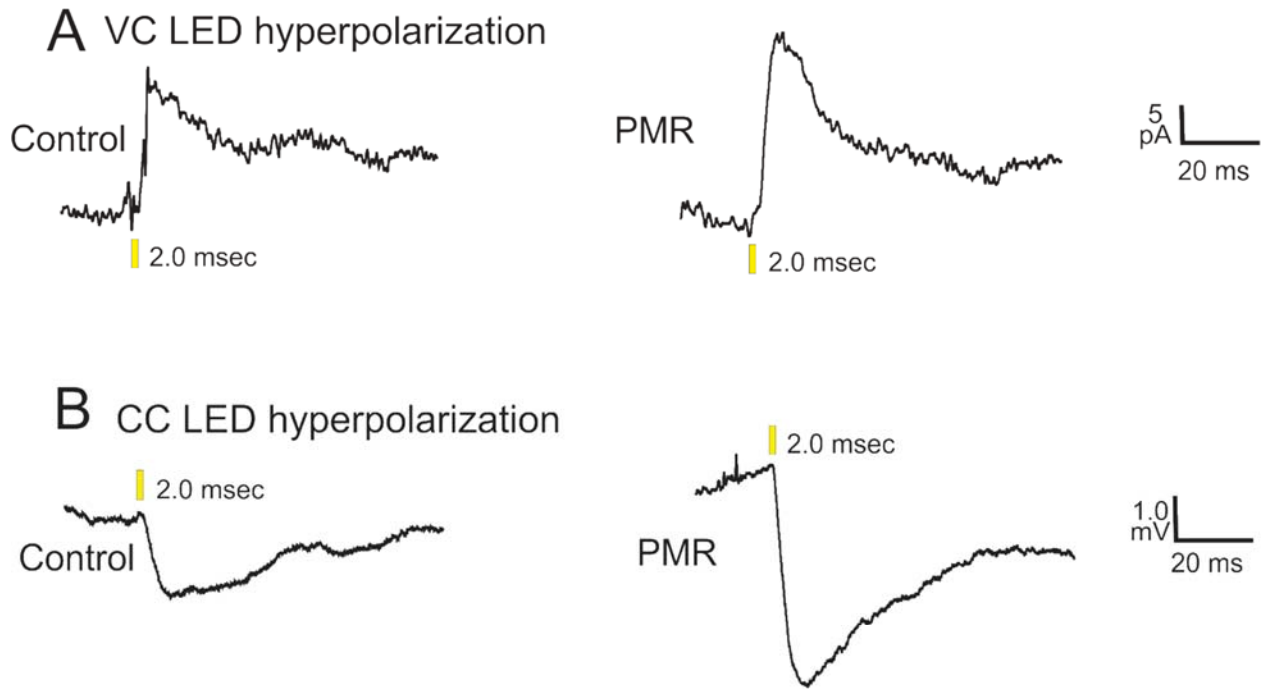


Figure 3.12 Examples of the effect of γ LED stimulation of SS neurons in control (left) and PMR (right) cortex containing Arch-SS neurons. **A** Voltage-clamp recording in A and current clamp recording in B. The γ LED stimulation was 2.0 msec long in all cases.

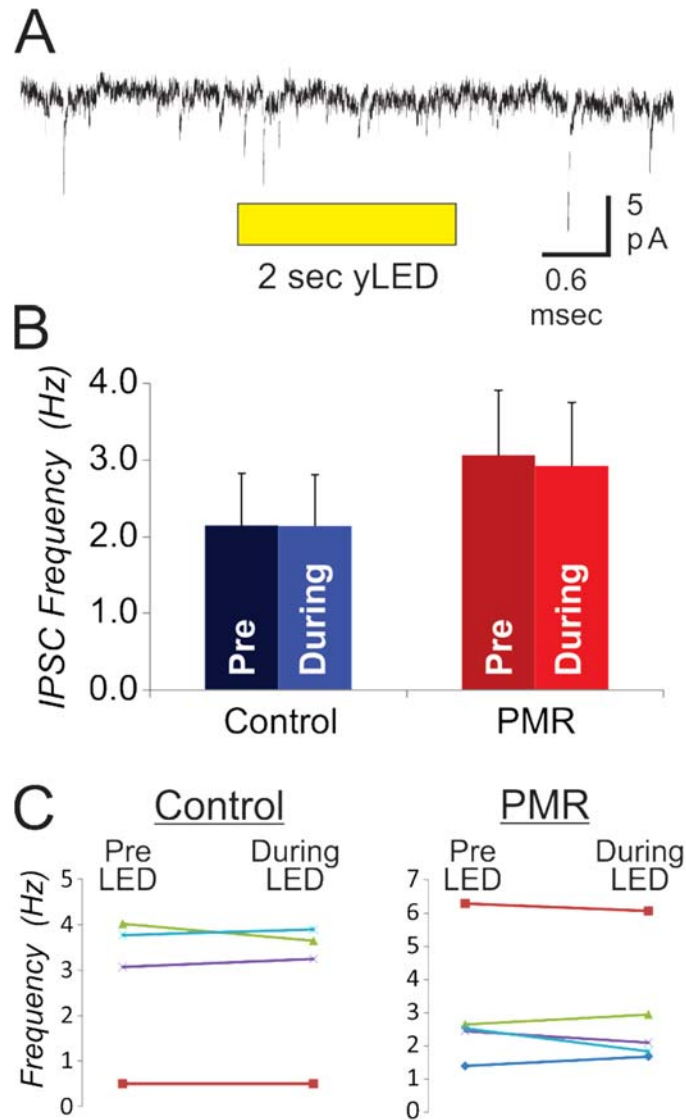


Figure 3.13 Spontaneous IPSCs recorded from pyramidal neurons before, during and after 2 sec yLED application in tissue containing Arch-SS neurons. **A.** Example of events during one of 20 trials recorded in this PMR neuron. **B.** Mean \pm SEM showed that even prior to the yLED application that IPSC frequency was very low. The yLED did not produce a significant effect on frequency measured over this 2 sec duration in 4 control and 5 PMR neurons (t-tests used to compare pre to during separately for each group, $p > 0.05$). **C.** Effect of the light on the frequencies of individual neurons (represented in different colors) for control (left) and PMR (right).

Chapter 4:

Discussion

The overall objective of this study was to assess whether cortical LTS interneurons function differently within freeze-lesion induced microgyric cortex using direct and selective cellular manipulation. Utilizing optogenetics in conjunction with whole cell patch clamping and field potential studies, the following observations were made: (1) the SS/LTS interneuron mediated evocation of IPSCs in layer V pyramidal neurons is more robust in PMR. Similarly, the data suggests that electrically-evoked IPSCs from layer V PMR pyramidal cells are larger than those evoked in control. (2) Data suggests that SS/LTS interneuron mediated suppression of electrically-evoked responses may be stronger in PMR; and (3) the selective silencing of SS/LTS interneurons might not impart an effect on spontaneous inhibitory postsynaptic events at low levels of network activity.

LTS interneurons were targeted in these studies due to previous work that identified these modulatory cells as potential contributors to the induction of epileptiform activity within PMR cortex. In this lab, preceding studies suggest that cortical LTS interneurons are possibly more active in the microgyric brain. These cells have been shown to receive three times the excitatory input control LTS interneurons have been demonstrated to receive (unpublished data). Moreover, group 1 mGluRs (mGluR₁ and mGluR₅), receptors that selectively excite LTS interneurons, display increased excitation in PMR. mGluR₅, which does not display activation in control cortex, has been demonstrated to have anomalous expression (established with western blotting) and activity within PMR (unpublished data). These indirectly posit that LTS may be more active

within PMR. Studies in this work were an attempt to assess this biologically and provide direct evidence of PMR LTS increased output.

Overactive LTS functionality may occur in conjunction to or possibly because of reductions in FS interneuron density in deep layers of cortex (layers V and VI) that persists in older animals, as determined by PV-immunostaining (Rosen et al. 1998). While it is possible that this reduced staining does not correspond with reductions of PV cellular population density or even inhibitory function, the established fact that overall levels of inhibition remain the same between control and PMR cortex as well as the suggested overactivity of LTS interneurons within PMR, indicates that this might be the case. Reduction of FS intralaminar inhibition in conjunction to a relative increase in LTS intracolumnar inhibition could induce increased and unchecked pyramidal neuron synchrony (Bush and Sejnowski 1996), the cellular basis of epileptic seizures (observed in this animal model as epileptiform activity).

This hypothesized mechanistic change seen with SS and PV interneurons may pathologically extend beyond just the induction of epilepsy and in fact, could induce other neurological issues such as developmental malformation-associated deficits in learning and memory. The freeze-lesion model used in these studies, in fact, has been found to impair the speed of auditory processing in rats and mice, a phenomenon associated with an elevated incidence of developmental dyslexia in humans (Threlkeld et al. 2007). SS-interneurons, and potentially also PV interneurons, functioning in such a vastly different way in malformed cortex, could potentially underlie such behavioral maldevelopment; therefore, elucidating these cellular mechanisms will offer insight into how secondary neurological abnormalities can arise, as well as provide means to potentially ameliorate the associated intractable epilepsy.

Evaluating LTS/SS in PMR with Channelrhodopsin2

Performing the freeze-lesion surgery in animals bred to express ChR2 or Arch specifically on their SS-containing cells, bearing in mind the 6-10% chance of ChR2 expression in PV-expressing cells (Hu et al. 2013), allowed us to selectively manipulate SS interneurons and observe that SS interneurons do seem to be more powerful modulators of layer V pyramidal neurons within PMR compared to control cortex. Evoked IPSCs recorded from layer V pyramidal neurons by the application of stimulating blue light were profoundly and consistently larger in PMR than those evoked in control. Given the robustness of this effect, studies performed after were expected to follow suit. However, the application of blue light during electrical-evocation of IPSCs, compared to IPSCs evoked with electrical alone, had interesting results. For these experiments, EPSC blockers were in bath solution, so while the electrical component was stimulating all cells in its vicinity, recordings from pyramidal neurons would only supply us with effects of inhibitory interneurons. In control pyramidal cells, electrically-evoked and electrical plus bLED-evoked IPSCs were not different; this is likely because SS/LTS interneurons are weaker in control cortex (Figure 1.1). bLED activation of them would not evoke an inhibitory response large enough to interfere with the electrically-evoked response. In PMR pyramidal cells, we believe that upon addition of more cells, electrical plus bLED will cause smaller responses than those caused by electrical alone. If the electrical component is truly activating all neurons in the vicinity, then this response demonstrates disinhibition. It is important to remember that cortical networks comprise many different interactive cell types. In this case, let us minimize to a three neuron circuit containing an SS/LTS interneuron, an FS/PV interneuron, and an excitatory pyramidal neuron (visualized in Figure 4.1). The pyramidal

neuron is receiving input from both LTS and FS. Even though FS population density in layer V is theoretically reduced, some FS remains and will function accordingly, albeit to a lesser collective degree. The FS synapsing onto the pyramidal neuron is receiving input itself from LTS (Gibson et al. 1999). Therefore, selective stimulation of LTS by bLED will inhibit both pyramidal and FS cells. When compared to an electrically-evoked IPSC, the inhibition of an inhibitory source (disinhibition) will, in this case, look like a smaller IPSC. This is supported by Figure 3.11D and E. Comparing control electrical plus bLED to the same in PMR suggests the possibility for smaller IPSCs in PMR pyramidal neurons. If the control data did comprise highest possible evoked IPSC peak (since bLED did not impart any reducing effect), then the only way for PMR values to be smaller is if PMR LTS interneurons are more powerful here. Following electrical activation, SS interneurons were still able to be activated, and were, by bLED. Their activation caused the relief of FS inhibition onto the patched pyramidal neuron, thereby reducing the amount of evoked IPSC to levels even smaller than those evoked in control (this is a pattern; not statistically significant; Figure 3.13E), wherein all cells are being activated without additional influence by LTS.

Disinhibition was also demonstrated in the performed field potential studies. The effect of bLED on the excitatory field was less in PMR than it was in controls. This seems backwards at first, particularly since bLED produces larger IPSCs in PMR pyramidal neurons, compared to controls (Figure 3.6). Intuitively, we expected application of bLED to suppress the electrically-evoked excitatory field potential in PMR, as it occurred in the control slice. As summarized above, however, LTS synapse onto FS interneurons as well as onto pyramidal neurons, so given their stronger influence in PMR (Figure 1.1), these cells may have increased their output onto FS, resulting in strong disinhibition. This causes increased network excitation by way of

electrically-stimulated pyramidal cell responsiveness overcoming the inhibition they are now receiving from just LTS interneurons alone.

Studies wherein bLED stimulation was applied at varying distances from the patched pyramidal cell reveal some interesting information about LTS distribution in PMR versus control cortex. The experiments comprised moving bLED stimulation horizontally within layer V, at lateral distances of 200 μm and 400 μm . Stimulation at these lateral distances significantly reduced the amplitude of IPSCs evoked in PMR. The percent of reduction appears to be greater for mid-level intensities than high intensities in control cells. In PMR, even high intensity stimulation at distant application sites does not produce an IPSC similar to that observed by bLED application directly over the neuron. Decreases in IPSC amplitudes in this manner are expected as the horizontal distance between recorded neuron and location of stimulation increases. This is because SS interneurons are typically intracolumnar (a column has a width of ~ 0.4 mm). The fact that this horizontal distance over which the SS-evoked IPSC can be produced is not greater in PMR than in control suggests that in PMR, the SS interneurons remain intracolumnar. In addition, it suggests that the increased output that the SS interneurons have in PMR cortex does not come from a horizontal spread of their axons.

At least some SS interneurons in layer II/III project to layer V and vice versa, so we expected to see some IPSC activity in layer V pyramidal neurons following bLED stimulation in layer II/III. We have established in this work that SS interneurons are more active within layer V PMR (Figure 3.6). As we know, SS interneurons orient their arbors vertically, within columns (Markram et al. 2004). The horizontal studies discussed above, demonstrate that SS interneurons remain intracolumnar, so these vertical-stimulation data should reveal information about their intracolumnar influence as it may be altered between control and PMR. And it does: when

comparing control and PMR for the conditions of layer V and layer II/III bLED stimulation, we believe that these non-significant data suggest a difference in the interaction between group and condition, signifying that effects may be greater in layer V than they are in layer II/III.

Additional comparison between IPSCs evoked by layer II/III stimulation in control versus PMR indicates that the two groups are not different in this parameter. This confirms that the effects seen in layer V are due to increased output by SS interneurons also in layer V as compared to output from layer II/III. These data are supported in part by studies published in 2010, wherein inhibitory input was increased in a region-specific manner in pyramidal cells in FL cortex, with layer V being more severely affected than layer II/III (Brill and Huguenard, 2010)

Evaluating LTS/SS in PMR with Archærhodopsin

The included Arch study, which evaluated the effect SS/LTS silencing has on spontaneous IPSCs, showed that the removal of SS-mediated inhibition does not impact the frequency of spontaneous inhibitory events. There are a few concerns with these data. It is possible that cellular activity under these conditions was too low for us to properly observe an effect (aCSF, as previously described; bath heated to 32°C; APV and DNQX). Given the frequency of IPSCs in the recordings, 1-2 Hz (one to two events per second), and the length of time per recording period (six seconds; two second pre-light, two seconds with yLED, and two seconds post-light), it would be difficult to ascertain if a reduction was truly taking place. Additionally, the induction of an IPSC event in a pyramidal neuron, under these conditions, would be from FS and LTS interneurons. These two cells create synapses onto different parts of postsynaptic neurons: FS interneurons synapse onto a neuron's soma, while LTS forms synapses onto neuron dendrites (Figure 4.1; Markram et al. 2004). This is important to consider when

establishing from where the bulk of IPSC in postsynaptic neurons comes from. All recordings took place within the pyramidal soma, so inhibitory events evoked by SS interneurons would have decayed by the time they propagate to soma from the dendrite. Because of this, the majority of recorded events would have been caused by FS cells and thusly, given the frequency level, too few of the events would have been evoked by LTS. Silencing them with yLED, would not yield a large reduction at this frequency.

To address this, we could lengthen the recording period. For example, if yLED silencing of SS-Arch interneurons evoked a 10% reduction in total IPSC frequency, then even if the frequency remained at 1-2 Hz, lengthening the recording period to 30 seconds pre-light, 30 seconds with light, and 30 seconds post-light would theoretically give more events evoked by LTS interneurons, to be potentially silenced upon exposure with yLED.

We could also modify the recording conditions to increase network activity, and therefore raise event frequency. This can be done by altering the concentrations of potassium ions, chloride, and/or magnesium ions in extracellular aCSF bath solution (3.5 mM K^+ , 1.2 mM Ca^+ , and 1.0 mM Mg^+ used in these experiments), increasing the temperature to cause neurons to become more active, or even by adding a small concentration of gabazine. Gabazine, a GABA_A antagonist, could be used at low levels to lessen inhibition resulting in a more active environment. Of course, it seems counter-intuitive to use an inhibitory event blocker when attempting to record inhibitory events, but at low enough concentrations, gabazine would modify network activity enough to promote the induction of spontaneous IPSCs, which would enable us to see any potential effects the silencing of SS/LTS interneurons might have on them.

Summary and future directions

To conclude, these series of *ex vivo* experiments revealed that LTS interneurons do impart a greater modulatory effect in layer V PMR cortex, as compared to control. This influence is not experienced exclusively by excitatory principle neurons, but by inhibitory interneurons as well, causing phenomena like increased disinhibition to occur upon selective, and noninvasive activation with light. Optogenetics enabled us to study these cells directly and with minimal disruption of neighboring cell types.

To quickly address the low n used within each group, it is important note that these studies are largely preliminary and were performed for the first time in the lab this past year, therefore problems with data collection and analysis prevented included groups from being too large. For the purposes of discussion and concept development, especially in regard to future directions, certain non-significant groups were not disregarded (due to low n). Still, the fact that statistical analyses of much of the included data read as significant, suggests that upon the addition of more cells, we would potentially see more strong differences.

Future studies, beyond ones mentioned in this work, could involve evaluation of the effect SS/LTS interneuron activation might have on electrically-evoked EPSCs recorded from layer V PMR pyramidal cells, as compared to control. It would be interesting to see if disinhibition comes into play under these conditions as well. Some preliminary evoked-EPSC experiments were performed previously. Protocol was the same used for evoked-IPSC data, but bath solution did not contain any EPSC-blocking agents. At higher electrical-intensities, there was a problem with the induction of action potentials, which confounded the sought information regarding EPSCs as they might be changed upon exposure with light. This can be addressed with the addition of QX-314, a sodium channel blocker.

It is possible to breed mice with optogenetic channels on PV/FS interneurons as well. Performing experiments wherein PV-ChR2 and PV-Arch mice are used would reveal even more information about PV interneuron functioning and how it might change in malformed cortex, especially given the amassed evidence suggesting LTS over-activity in layer V PMR.

Given previous implications of SS/LTS interneuron epileptiform activity-promoting alterations in PMR cortex, in SS-ChR2 tissue, bLED-alone stimulation intensity series was employed to assess whether it was possible to not only induce epileptiform discharges electrically, but with selective SS interneuron activation (bath contained 0.02 mM gabazine). Shown is the all-or-none ictal-like response as induced by two millisecond durations of bLED (Figure 4.2). This is the first biological example of SS/LTS activation causing epileptiform activity this lab has demonstrated in this model; however, this was only performed in PMR tissue. Upon continuation of these studies, this experiment should be replicated in control tissue to demonstrate whether the activation of SS interneurons truly is sufficient to initiate epileptiform activity within PMR.

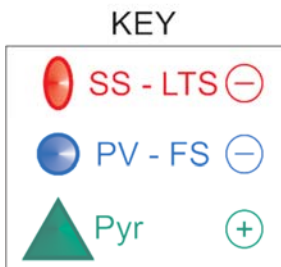
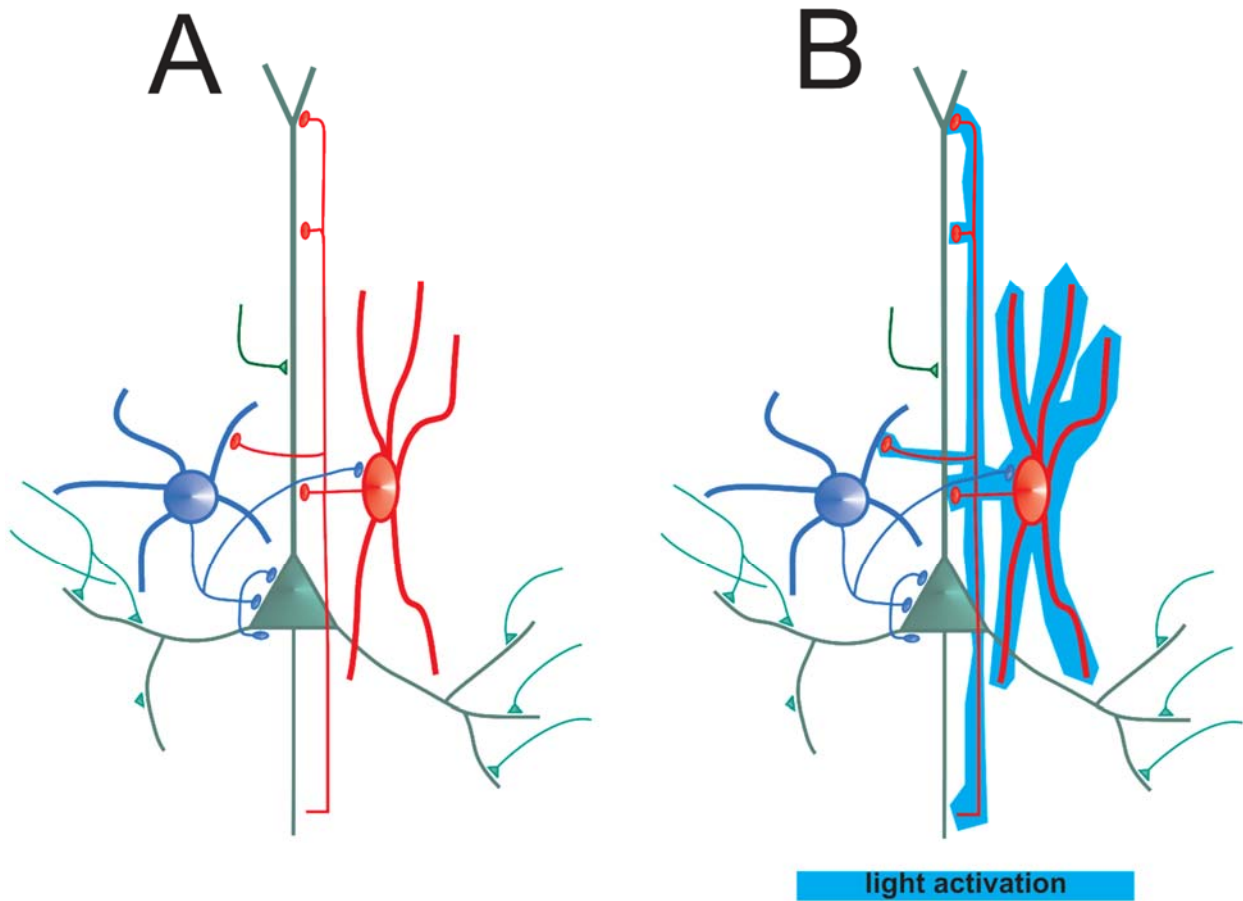


Figure 4.1 Model visualizing the orientation of and interactions between the three neuron types focused on in this writing.

SS: Somatostatin, corresponding with inhibitory (-) dendrite-targeting LTS interneurons
 PV: Parvalbumin, corresponding with inhibitory (-) soma-targeting FS interneurons
 Pyr: Pyramidal, corresponding with excitatory (+) principle neurons

A: As is shown: SS interneurons synapse onto Pyr and FS and FS interneurons synapse onto Pyr and to a lesser degree, SS.

B: Blue halo around SS represents bLED activation. γ LED inhibition could be represented the same way.

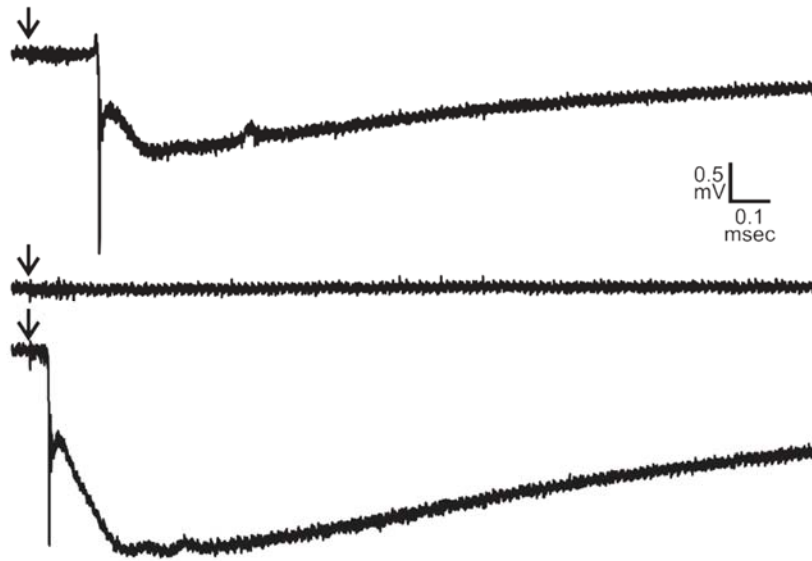


Figure 4.2 Example of activation of ictal activity with bLED in PMR cortex containing ChR-SS neurons. The aCSF bath contains 0.02 mM gabazine. Three successive stimuli (2 msec bLED duration). This all-or-none ictal-like activity did not occur spontaneously (without light) nor when yellow light was applied. Thus this is the first biological example of what our computational model previously showed, that epileptiform activity can be initiated when SS neurons are activated in PMR cortex.

List of References

- (1984). Cerebral Cortex: Cellular Components of the Cerebral Cortex; Vol 1. New York, Plenum Publishing Corp.
- (1989). "Proposal for revised classification of epilepsies and epileptic syndromes. Commission on Classification and Terminology of the International League Against Epilepsy." Epilepsia **30**(4): 389-399.
- Adesnik, H., W. Bruns, H. Taniguchi, Z. J. Huang and M. Scanziani (2012). "A neural circuit for spatial summation in visual cortex." Nature **490**(7419): 226-231.
- Araujo, D., D. B. de Araujo, O. M. Pontes-Neto, S. Escorsi-Rosset, G. N. Simao, L. Wichert-Ana, T. R. Velasco, A. C. Sakamoto, J. P. Leite and A. C. Santos (2006). "Language and motor fMRI activation in polymicrogyric cortex." Epilepsia **47**(3): 589-592.
- Atallah, B. V., W. Bruns, M. Carandini and M. Scanziani (2012). "Parvalbumin-expressing interneurons linearly transform cortical responses to visual stimuli." Neuron **73**(1): 159-170.
- Bacci, A. and J. R. Huguenard (2006). "Enhancement of spike-timing precision by autaptic transmission in neocortical inhibitory interneurons." Neuron **49**(1): 119-130.
- Bacci, A., J. R. Huguenard and D. A. Prince (2004). "Long-lasting self-inhibition of neocortical interneurons mediated by endocannabinoids." Nature **431**(7006): 312-316.
- Bacci, A., U. Rudolph, J. R. Huguenard and D. A. Prince (2003). "Major differences in inhibitory synaptic transmission onto two neocortical interneuron subclasses." J Neurosci **23**(29): 9664-9674.
- Balcells Riba, M. (1999). "[Contribution of John Hughlings Jackson to the understanding of epilepsy]." Neurologia **14**(1): 23-28.
- Barkovich, A. J. (2010). "Current concepts of polymicrogyria." Neuroradiology **52**(6): 479-487.
- Barkovich, A. J., R. Hevner and R. Guerrini (1999). "Syndromes of bilateral symmetrical polymicrogyria." AJNR Am.J.Neuroradiol. **20**(10): 1814-1821.
- Barkovich, A. J. and B. O. Kjos (1992). "Gray matter heterotopias: MR characteristics and correlation with developmental and neurologic manifestations." Radiology **182**: 493-499.
- Barkovich, A. J. and B. O. Kjos (1992). "Nonlissencephalic cortical dysplasias: correlation of imaging findings with clinical deficits." AJNR.Am.J.Neuroradiol. **13**: 95-103.
- Berkovic, S. F., J. C. Mulley, I. E. Scheffer and S. Petrou (2006). "Human epilepsies: interaction of genetic and acquired factors." Trends Neurosci. **29**(7): 391-397.

- Bladin, C. F., A. V. Alexandrov, A. Bellavance, N. Bornstein, B. Chambers, R. Cote, L. Lebrun, A. Pirisi and J. W. Norris (2000). "Seizures after stroke: a prospective multicenter study." Arch.Neurol. **57**(11): 1617-1622.
- Blumcke, I., H. V. Vinters, D. Armstrong, E. Aronica, M. Thom and R. Spreafico (2009). "Malformations of cortical development and epilepsies: neuropathological findings with emphasis on focal cortical dysplasia." Epileptic.Disord. **11**(3): 181-193.
- Brill J., Huguenard J. R. (2010). "Enhanced Infragranular and Supragranular Synaptic Input onto Layer 5 Pyramidal Neurons in a Rat Model of Cortical Dysplasia." Cerebral Cortex. **20**(12): 2926-2938.
- Buckmaster, P. S. and F. E. Dudek (1997). "Neuron loss, granule cell axon reorganization, and functional changes in the dentate gyrus of epileptic kainate-treated rats." J.Comp Neurol. **385**(3): 385-404.
- Buhl, E. H., G. Tamas, T. Szilagy, C. Stricker, O. Paulsen and P. Somogyi (1997). "Effect, number and location of synapses made by single pyramidal cells onto aspiny interneurons of cat visual cortex." Journal of Physiology (Cambridge, Eng.) **500 (Pt 3)**: 689-713.
- Bush, P. and T. Sejnowski (1996). "Inhibition synchronizes sparsely connected cortical neurons within and between columns in realistic network models." Journal of Computational Neuroscience **3**(2): 91-110.
- Cardin, J. A., M. Carlen, K. Meletis, U. Knoblich, F. Zhang, K. Deisseroth, L. H. Tsai and C. I. Moore (2009). "Driving fast-spiking cells induces gamma rhythm and controls sensory responses." Nature **459**(7247): 663-667.
- Cauli, B., E. Audinat, B. Lambolez, M. C. Angulo, N. Ropert, K. Tsuzuki, S. Hestrin and J. Rossier (1997). "Molecular and physiological diversity of cortical nonpyramidal cells." J Neurosci **17**: 3894-3906.
- Cepeda, C., V. M. Andre, M. S. Levine, N. Salamon, H. Miyata, H. V. Vinters and G. W. Mathern (2006). "Epileptogenesis in pediatric cortical dysplasia: the dysmature cerebral developmental hypothesis." Epilepsy Behav. **9**(2): 219-235.
- Chassoux, F., E. Landre, S. Rodrigo, F. Beuvon, B. Turak, F. Semah and B. Devaux (2008). "Intralesional recordings and epileptogenic zone in focal polymicrogyria." Epilepsia **49**(1): 51-64.
- Chow, B. Y., X. Han, A. S. Dobry, X. F. Qian, A. S. Chuong, M. J. Li, M. A. Henninger, G. M. Belfort, Y. X. Lin, P. E. Monahan and E. S. Boyden (2010). "High-performance genetically targetable optical neural silencing by light-driven proton pumps." Nature **463**(7277): 98-102.
- Colmers, W. F. and B. El Bahh (2003). "Neuropeptide Y and Epilepsy." Epilepsy Curr. **3**(2): 53-58.

Crick, F. (1999). "The impact of molecular biology on neuroscience." Philosophical Transactions of the Royal Society of London Series B-Biological Sciences **354**(1392): 2021-2025.

Crome, L. (1952). "Microgyria." J Path Bact **64**: 479-495.

de Leon, G. A. (1972). "Observations on cerebral and cerebellar microgyria." Acta Neuropathol.(Berl) **20**: 278-287.

Defazio, R. A. and J. J. Hablitz (1999). "Reduction of Zolpidem Sensitivity in a Freeze Lesion Model of Neocortical Dysgenesis." Journal of Neurophysiology **81**(1): 404-407.

Defazio, R. A. and J. J. Hablitz (2000). "Alterations in NMDA receptors in a rat model of cortical dysplasia." J Neurophysiol **83**: 315-321.

Deisseroth, K., G. P. Feng, A. K. Majewska, G. Miesenbock, A. Ting and M. J. Schnitzer (2006). "Next-generation optical technologies for illuminating genetically targeted brain circuits." Journal of Neuroscience **26**(41): 10380-10386.

Dichter, M. A. and G. F. Ayala (1987). "Cellular mechanisms of epilepsy: A status report." Science **237**: 157-164.

Dinocourt, C., Z. Petanjek, T. F. Freund, Y. Ben Ari and M. Esclapez (2003). "Loss of interneurons innervating pyramidal cell dendrites and axon initial segments in the CA1 region of the hippocampus following pilocarpine-induced seizures." J.Comp Neurol. **459**(4): 407-425.

Dua, T., H. M. De Boer and L. L. Prilipko (2005). "Atlas: Epilepsy care in the world." Epilepsia **46**: 28-28.

Dvorak, K. and J. Feit (1977). "Migration of neuroblasts through partial necrosis of the cerebral cortex in newborn rats. Contribution to the problems of morphological development and developmental period of cerebral microgyria." Acta Neuropathol **38**: 203-212.

Dvorak, K., J. Feit and Z. Jurankova (1978). "Experimentally induced focal microgyria and status verrucosus deformis in rats. Pathogenesis and interrelation histological and autoradiographical study." Acta Neuropathol **44**: 121-129.

Eadie, M. J. and P. F. Bladin (2001). A Disease Once Sacred, A History of the Medical Understanding of Epilepsy. England, John Libbey and Co., LTD.

Fairen, A., J. DeFelipe and J. Regidor (1984). Nonpyramidal Neurons: general account. Cerebral Cortex. E. G. Jones and A. Peters. New York, Plenum: 201-245.

Fasulo, L., S. Saucedo, L. Caceres, S. Solis and R. Caraballo (2012). "Migrating Focal Seizures During Infancy: A Case Report and Pathologic Study." Pediatric Neurology **46**(3): 182-184.

- Fenko, L., O. Yizhar and K. Deisseroth (2011). "The Development and Application of Optogenetics." Annual Review of Neuroscience, Vol 34 **34**: 389-412.
- Flint, A. C. and A. R. Kriegstein (1997). "Mechanisms underlying neuronal migration disorders and epilepsy." Curr.Opin.Neurol. **10**: 92-97.
- Frey, L. C. (2003). "Epidemiology of posttraumatic epilepsy: a critical review." Epilepsia **44 Suppl 10**: 11-17.
- Fricker, D. and R. Miles (2001). "Interneurons, spike timing, and perception." Neuron **32**(5): 771-774.
- Geiger, J. R., J. Lnbke, A. Roth, M. Frotscher and P. Jonas (1997). "Submillisecond AMPA receptor-mediated signaling at a principal neuron-interneuron synapse." Neuron **18**(6): 1009-1023.
- Giannetti, S., P. Gaglini, F. Di Rocco, C. Di Rocco and A. Granato (2000). "Organization of cortico-cortical associative projections in a rat model of microgyria." Neuroreport **11**(10): 2185-2189.
- Giannetti, S., P. Gaglini, A. Granato and C. Di Rocco (1999). "Organization of callosal connections in rats with experimentally induced microgyria." Childs Nerv.Syst. **15**(9): 444-448.
- Gibson, J. R., M. Beierlein and B. W. Connors (1999). "Two networks of electrically coupled inhibitory neurons in neocortex." Nature **402**: 75-79.
- Guerrini, R. and R. Carrozzo (2002). "Epileptogenic brain malformations: clinical presentation, malformative patterns and indications for genetic testing." Seizure. **11 Suppl A**: 532-543.
- Guerrini, R. and T. Filippi (2005). "Neuronal migration disorders, genetics, and epileptogenesis." J.Child Neurol. **20**(4): 287-299.
- Guerrini, R., F. Sicca and L. Parmeggiani (2003). "Epilepsy and malformations of the cerebral cortex." Epileptic.Disord. **5 Suppl 2**: S9-26.
- Hauser, W. A. (1998). Epilepsy, A Comprehensive Textbook. Philadelphia, Lippincott-Raven.
- Hayashi, N., Y. Tsutsumi and A. J. Barkovich (2002). "Polymicrogyria without porencephaly/schizencephaly. MRI analysis of the spectrum and the prevalence of macroscopic findings in the clinical population." Neuroradiology **44**(8): 647-655.
- Hestrin, S. (1993). "Different glutamate receptor channels mediate fast excitatory synaptic currents in inhibitory and excitatory cortical neurons." Neuron **11**: 1083-1091.

Houser, C. R., S. H. Hendry, E. G. Jones and J. E. Vaughn (1983). "Morphological diversity of immunocytochemically identified GABA neurons in the monkey sensory-motor cortex." J.Neurocytol. **12**: 617-638.

Hu, H., J. Z. Cavendish and A. Agmon (2013). "Not all that glitters is gold: off-target recombination in the somatostatin-IRES-Cre mouse line labels a subset of fast-spiking interneurons." Front Neural Circuits **7**: 195.

Humphreys, P., G. D. Rosen, D. M. Press, G. F. Sherman and A. M. Galaburda (1991). "Freezing lesions of the developing rat brain: A model for cerebrocortical microgyria." J.Neuropathol.Exp.Neurol. **50**: 145-160.

Jacobs, K. M., M. J. Gutnick and D. A. Prince (1996). "Hyperexcitability in a model of cortical maldevelopment." Cereb Cortex **6**(3): 514-523.

Jacobs, K. M., B. J. Hwang and D. A. Prince (1999a). "Focal epileptogenesis in a rat model of polymicrogyria." Journal of Neurophysiology **81**: 159-173.

Jacobs, K. M., V. N. Kharazia and D. A. Prince (1999b). "Mechanisms underlying epileptogenesis in cortical malformations." Epilepsy Research **36**: 165-188.

Jacobs, K. M., M. Mogensen, L. Warren and D. A. Prince (1999c). "Experimental microgyria disrupt the barrel field pattern in rat somatosensory cortex." Cerebral Cortex **9**(7): 733-744.

Jacobs, K. M. and D. A. Prince (2005). "Excitatory and inhibitory postsynaptic currents in a rat model of epileptogenic microgyria." J Neurophysiol. **93**(2): 687-696.

Jallon, P., P. Loiseau and J. Loiseau (2001). "Newly diagnosed unprovoked epileptic seizures: presentation at diagnosis in CAROLE study. Coordination Active du Réseau Observatoire Longitudinal de l'Épilepsie." Epilepsia **42**(4): 464-475.

Kawaguchi, Y. (1993). "Groupings of nonpyramidal and pyramidal cells with specific physiological and morphological characteristics in rat frontal cortex." Journal of Neurophysiology **69**: 416-431.

Kawaguchi, Y. and S. Kondo (2002). "Parvalbumin, somatostatin and cholecystokinin as chemical markers for specific GABAergic interneuron types in the rat frontal cortex." J Neurocytol. **31**(3-5): 277-287.

Kawaguchi, Y. and Y. Kubota (1993). "Correlation of physiological subgroupings of nonpyramidal cells with parvalbumin- and calbindinD28k-immunoreactive neurons in layer V of rat frontal cortex." Journal of Neurophysiology **70**: 387-396.

Kawaguchi, Y. and Y. Kubota (1997). "GABAergic cell subtypes and their synaptic connections in rat frontal cortex." Cereb.Cortex **7**(6): 476-486.

- Kellinghaus, C., G. Moddel, H. Shigeto, Z. Ying, B. Jacobsson, J. Gonzalez-Martinez, C. Burrier, D. Janigro and I. M. Najm (2007). "Dissociation between in vitro and in vivo epileptogenicity in a rat model of cortical dysplasia." Epileptic.Disord. **9**(1): 11-19.
- Klaassen, A., J. Glykys, J. Maguire, C. Labarca, I. Mody and J. Boulter (2006). "Seizures and enhanced cortical GABAergic inhibition in two mouse models of human autosomal dominant nocturnal frontal lobe epilepsy." Proc.Natl.Acad.Sci.U.S.A **103**(50): 19152-19157.
- Kuhlman, S. J. and Z. J. Huang (2008). "High-Resolution Labeling and Functional Manipulation of Specific Neuron Types in Mouse Brain by Cre-Activated Viral Gene Expression." Plos One **3**(4).
- Kvitsiani, D., S. Ranade, B. Hangya, H. Taniguchi, J. Z. Huang and A. Kepecs (2013). "Distinct behavioural and network correlates of two interneuron types in prefrontal cortex." Nature **498**(7454): 363-+.
- Kwan, P. and M. J. Brodie (2006). "Combination therapy in epilepsy - When and what to use." Drugs **66**(14): 1817-1829.
- Laurie, D. J., W. Wisden and P. H. Seeburg (1992). "The distribution of thirteen GABAA receptor subunit mRNAs in the rat brain. III. Embryonic and postnatal development." J.Neurosci. **12**: 4151-4172.
- Ledri, M., M. G. Madsen, L. Nikitidou, D. Kirik and M. Kokaia (2014). "Global Optogenetic Activation of Inhibitory Interneurons during Epileptiform Activity." Journal of Neuroscience **34**(9): 3364-3377.
- Lee, K. S., F. Schottler, J. L. Collins, G. Lanzino, D. Couture, A. Rao, K. Hiramatsu, Y. Goto, S. C. Hong, H. Caner, H. Yamamoto, Z. F. Chen, E. Bertram, S. Berr, R. Omary, H. Scrabble, T. Jackson, J. Goble and L. Eisenman (1997). "A genetic animal model of human neocortical heterotopia associated with seizures." J.Neurosci. **17**: 6236-6242.
- Leventer, R. J., R. Guerrini and W. B. Dobyns (2008). "Malformations of cortical development and epilepsy." Dialogues.Clin.Neurosci. **10**(1): 47-62.
- Lim, C. C., H. Yin, N. K. Loh, V. G. Chua, F. Hui and A. J. Barkovich (2005). "Malformations of cortical development: high-resolution MR and diffusion tensor imaging of fiber tracts at 3T." AJNR Am.J.Neuroradiol. **26**(1): 61-64.
- Lin, W. C., C. M. Davenport, A. Mourot, D. Vytla, C. M. Smith, K. A. Medeiros, J. J. Chambers and R. H. Kramer (2014). "Engineering a light-regulated GABAA receptor for optical control of neural inhibition." ACS Chem Biol **9**(7): 1414-1419.

Luhmann, H. J., K. Raabe, M. Qu and K. Zilles (1998). "Characterization of neuronal migration disorders in neocortical structures: extracellular in vitro recordings." European Journal of Neuroscience **10**: 3085-3094.

Maccaferri, G. and J. C. Lacaille (2003). "Interneuron Diversity series: Hippocampal interneuron classifications--making things as simple as possible, not simpler." Trends Neurosci. **26**(10): 564-571.

Madisen, L., T. Y. Mao, H. Koch, J. M. Zhuo, A. Berenyi, S. Fujisawa, Y. W. A. Hsu, A. J. Garcia, X. Gu, S. Zanella, J. Kidney, H. Gu, Y. M. Mao, B. M. Hooks, E. S. Boyden, G. Buzsaki, J. M. Ramirez, A. R. Jones, K. Svoboda, X. Han, E. E. Turner and H. K. Zeng (2012). "A toolbox of Cre-dependent optogenetic transgenic mice for light-induced activation and silencing." Nature Neuroscience **15**(5): 793-802.

Mann, E. O. and I. Mody (2008). "The multifaceted role of inhibition in epilepsy: seizure-genesis through excessive GABAergic inhibition in autosomal dominant nocturnal frontal lobe epilepsy." Curr.Opin.Neurol. **21**(2): 155-160.

Marin, O. (2012). "Interneuron dysfunction in psychiatric disorders." Nature Reviews Neuroscience **13**(2): 107-120.

Markram, H., M. Toledo-Rodriguez, Y. Wang, A. Gupta, G. Silberberg and C. Wu (2004). "Interneurons of the neocortical inhibitory system." Nat.Rev.Neurosci. **5**(10): 793-807.

Markram, H., Y. Wang and M. Tsodyks (1998). "Differential signaling via the same axon of neocortical pyramidal neurons." Proc.Natl.Acad.Sci.U.S.A **95**(9): 5323-5328.

Massengill, J. L., M. A. Smith, D. I. Son and D. K. O'Dowd (1997). "Differential expression of K4-AP currents and Kv3.1 potassium channel transcripts in cortical neurons that develop distinct firing phenotypes." J.Neurosci. **17**: 3136-3147.

McBain, C. J. and A. Fisahn (2001). "Interneurons unbound." Nat.Rev.Neurosci. **2**: 11-23.

McCormick, D. A., B. W. Connors, J. W. Lighthall and D. A. Prince (1985). "Comparative electrophysiology of pyramidal and sparsely spiny stellate neurons of the neocortex." Journal of Neurophysiology **54**: 782-806.

Miles, R. and J. C. Poncer (1993). "Metabotropic glutamate receptors mediate a post-tetanic excitation of guinea-pig hippocampal inhibitory neurones." J.Physiol.(Lond) **463**: 461-473.

Mirski, M. A. and P. N. Varelas (2008). "Seizures and status epilepticus in the critically ill." Crit Care Clin. **24**(1): 115-147, ix.

Montenegro, M. A., M. M. Guerreiro, I. Lopes-Cendes, C. A. Guerreiro and F. Cendes (2002). "Interrelationship of genetics and prenatal injury in the genesis of malformations of cortical development." Arch.Neurol. **59**(7): 1147-1153.

- Nagel, G., M. Brauner, J. F. Liewald, N. Adeishvili, E. Bamberg and A. Gottschalk (2005). "Light activation of channelrhodopsin-2 in excitable cells of *Caenorhabditis elegans* triggers rapid Behavioral responses." Current Biology **15**(24): 2279-2284.
- Nagel, G., T. Szellas, W. Huhn, S. Kateriya, N. Adeishvili, P. Berthold, D. Ollig, P. Hegemann and E. Bamberg (2003). "Channelrhodopsin-2, a directly light-gated cation-selective membrane channel." Proc Natl Acad Sci U S A **100**(24): 13940-13945.
- Osawa, S., M. Iwasaki, R. Hosaka, Y. Matsuzaka, H. Tomita, T. Ishizuka, E. Sugano, E. Okumura, H. Yawo, N. Nakasato, T. Tominaga and H. Mushiake (2013). "Optogenetically Induced Seizure and the Longitudinal Hippocampal Network Dynamics." Plos One **8**(4).
- Pascual-Castroviejo, I., S. I. Pascual-Pascual, J. Viaño, V. Martinez and R. Palencia (2001). "Unilateral polymicrogyria: a common cause of hemiplegia of prenatal origin." Brain and Development **23**(4): 216-222.
- Patrick, S. L., B. W. Connors and C. E. Landisman (2006). "Developmental changes in somatostatin-positive interneurons in a freeze-lesion model of epilepsy." Epilepsy Res. **70**(2-3): 161-171.
- Petreaanu, L., D. Huber, A. Sobczyk and K. Svoboda (2007). "Channelrhodopsin-2-assisted circuit mapping of long-range callosal projections." Nature Neuroscience **10**(5): 663-668.
- Pi, H. J., B. Hangya, D. Kvitsiani, J. I. Sanders, Z. J. Huang and A. Kepecs (2013). "Cortical interneurons that specialize in disinhibitory control." Nature **503**(7477): 521-+.
- Prince, D. A. and K. Jacobs (1998). "Inhibitory function in two models of chronic epileptogenesis." Epilepsy Research **32**(1-2): 83-92.
- Rakic, P. and P. J. Lombroso (1998). "Development of the cerebral cortex: I. Forming the cortical structure." J.Am.Acad.Child Adolesc.Psychiatry **37**(1): 116-117.
- Redecker, C., H. J. Luhmann, G. Hagemann, J. M. Fritschy and O. W. Witte (2000). "Differential downregulation of GABAA receptor subunits in widespread brain regions in the freeze-lesion model of focal cortical malformations." J Neurosci **20**: 5045-5053.
- Reyes, A., R. Lujan, A. Rozov, N. Burnashev, P. Somogyi and B. Sakmann (1998). "Target-cell-specific facilitation and depression in neocortical circuits." Nat Neurosci **1**(4): 279-285.
- Rivera, C., J. Voipio, J. A. Payne, E. Ruusuvuori, H. Lahtinen, K. Lamsa, U. Pirvola, M. Saarma and K. Kaila (1999). "The K⁺/Cl⁻ co-transporter KCC2 renders GABA hyperpolarizing during neuronal maturation [see comments]." Nature **397**(6716): 251-255.
- Rosen, G. D., D. Burstein and A. M. Galaburda (2000). "Changes in efferent and afferent connectivity in rats with induced cerebrocortical microgyria." J Comp Neurol **418**: 423-440.

- Rosen, G. D., K. M. Jacobs and D. A. Prince (1998). "Effects of neonatal freeze lesions on expression of parvalbumin in rat neocortex." Cereb.Cortex **8**(8): 753-761.
- Rosen, G. D., B. Mesples, M. Hendriks and A. M. Galaburda (2006). "Histometric changes and cell death in the thalamus after neonatal neocortical injury in the rat." Neuroscience **Epub ahead of print**.
- Rosen, G. D., D. M. Press, G. F. Sherman and A. M. Galaburda (1992). "The development of induced cerebrocortical microgyria in the rat." J.Neuropathol.Exp.Neurol. **51**: 601-611.
- Rosen, G. D., G. F. Sherman and A. M. Galaburda (1996). "Birthdates of neurons in induced microgyria." Brain Res. **727**: 71-78.
- Royer, S., B. V. Zemelman, A. Losonczy, J. Kim, F. Chance, J. C. Magee and G. Buzsaki (2012). "Control of timing, rate and bursts of hippocampal place cells by dendritic and somatic inhibition." Nature Neuroscience **15**(5): 769-775.
- Scantlebury, M. H., P. L. Ouellet, C. Psarropoulou and L. Carmant (2004). "Freeze lesion-induced focal cortical dysplasia predisposes to atypical hyperthermic seizures in the immature rat." Epilepsia **45**(6): 592-600.
- Schuele, S. U. and H. O. Luders (2008). "Intractable epilepsy: management and therapeutic alternatives." Lancet Neurol. **7**(6): 514-524.
- Sedel, F., I. Gourfinkel-An, O. Lyon-Caen, M. Baulac, J. M. Saudubray and V. Navarro (2007). "Epilepsy and inborn errors of metabolism in adults: a diagnostic approach." J.Inherit.Metab Dis. **30**(6): 846-854.
- Singer, W. (1999). "Neuronal synchrony: a versatile code for the definition of relations?" Neuron **24**(1): 49-25.
- Sisodiya, S. M. (2000). "Surgery for malformations of cortical development causing epilepsy." Brain **123 (Pt 6)**: 1075-1091.
- Sisodiya, S. M. (2004). "Malformations of cortical development: burdens and insights from important causes of human epilepsy." Lancet Neurol. **3**(1): 29-38.
- Somogyi, P. (1977). "A specific 'axo-axonal' interneuron in the visual cortex of the rat." Brain Res. **136**(2): 345-350.
- Somogyi, P., G. Tamas, R. Lujan and E. H. Buhl (1998). "Salient features of synaptic organisation in the cerebral cortex." Brain Res.Brain Res.Rev. **26**(2-3): 113-135.
- Sukhotinsky, I., A. M. Chan, O. J. Ahmed, V. R. Rao, V. Gradinaru, C. Ramakrishnan, K. Deisseroth, A. K.

Majewska and S. S. Cash (2013). "Optogenetic Delay of Status Epilepticus Onset in an In Vivo Rodent Epilepsy Model." Plos One **8**(4).

Super, H., S. P. Perez and E. Soriano (1997). "Survival of Cajal-Retzius cells after cortical lesions in newborn mice: a possible role for Cajal-Retzius cells in brain repair." Brain Res.Dev.Brain Res. **98**: 9-14.

Szydlowski, S. N., I. P. Dorocic, H. Planert, M. Carlen, K. Meletis and G. Silberberg (2013). "Target Selectivity of Feedforward Inhibition by Striatal Fast-Spiking Interneurons." Journal of Neuroscience **33**(4): 1678-1683.

Takanashi, J., H. Oba, A. J. Barkovich, H. Tada, Y. Tanabe, H. Yamanouchi, S. Fujimoto, M. Kato, M. Kawatani, A. Sudo, H. Ozawa, T. Okanishi, M. Ishitobi, Y. Maegaki and Y. Koyasu (2006). "Diffusion MRI abnormalities after prolonged febrile seizures with encephalopathy." Neurology **66**(9): 1304-1309.

Threlkeld, S.W., McClure M.M, Bai, J., Wang, Y., LoTurco, J.J., Rosen G.D., Fitch R.H. (2007). "Developmental disruptions and behavioral impairments in rats following in utero RNAi of *Dyx1c1*." Brain Res Bull **71**(5): 508-514.

Tsunematsu, T., T. S. Kilduff, E. S. Boyden, S. Takahashi, M. Tominaga and A. Yamanaka (2011). "Acute Optogenetic Silencing of Orexin/Hypocretin Neurons Induces Slow-Wave Sleep in Mice." Journal of Neuroscience **31**(29): 10529-10539.

Tsunematsu, T., S. Tabuchi, K. F. Tanaka, E. S. Boyden, M. Tominaga and A. Yamanaka (2013). "Long-lasting silencing of orexin/hypocretin neurons using archaerhodopsin induces slow-wave sleep in mice." Behavioural Brain Research **255**: 64-74.

Van Quyen, M. L., V. Navarro, J. Martinerie, M. Baulac and F. J. Varela (2003). "Toward a neurodynamical understanding of ictogenesis." Epilepsia **44**: 30-43.

Wang, X. J., B. M. Hooks and Q. Q. Sun (2014). "Thorough GABAergic innervation of the entire axon initial segment revealed by an optogenetic 'laserspritzer'." Journal of Physiology-London **592**(19): 4257-4276.

Wang, Y., A. Gupta, M. Toledo-Rodriguez, C. Z. Wu and H. Markram (2002). "Anatomical, physiological, molecular and circuit properties of nest basket cells in the developing somatosensory cortex." Cereb Cortex **12**(4): 395-410.

Wang, Y., M. Toledo-Rodriguez, A. Gupta, C. Wu, G. Silberberg, J. Luo and H. Markram (2004). "Anatomical, physiological and molecular properties of Martinotti cells in the somatosensory cortex of the juvenile rat." J Physiol **561**(Pt 1): 65-90.

Wilson, N. R., C. A. Runyan, F. L. Wang and M. Sur (2012). "Division and subtraction by distinct cortical inhibitory networks in vivo." Nature **488**(7411): 343-348.

- Wyllie, E. (2000). "Surgical treatment of epilepsy in pediatric patients." Can.J Neurol.Sci. **27**(2): 106-110.
- Xiang, Z., J. R. Huguenard and D. A. Prince (2002). "Synaptic inhibition of pyramidal cells evoked by different interneuronal subtypes in layer v of rat visual cortex." J Neurophysiol. **88**(2): 740-750.
- Xu, H., H. Y. Jeong, R. Tremblay and B. Rudy (2013). "Neocortical Somatostatin-Expressing GABAergic Interneurons Disinhibit the Thalamorecipient Layer 4." Neuron **77**(1): 155-167.
- Yizhar, O., L. E. Fenno, M. Prigge, F. Schneider, T. J. Davidson, D. J. O'Shea, V. S. Sohal, I. Goshen, J. Finkelstein, J. T. Paz, K. Stehfest, R. Fudim, C. Ramakrishnan, J. R. Huguenard, P. Hegemann and K. Deisseroth (2011). "Neocortical excitation/inhibition balance in information processing and social dysfunction." Nature **477**(7363): 171-178.
- Zilles, K., M. Qu, A. Schleicher and H. J. Luhmann (1998). "Characterization of neuronal migration disorders in neocortical structures: quantitative receptor autoradiography of ionotropic glutamate, GABA(A) and GABA(B) receptors." European Journal of Neuroscience **10**: 3095-3106.
- Zsombok, A. and K. M. Jacobs (2005). "Postsynaptic currents in layer iv neurons of epileptogenic malformed ferret cortex." Society for Neuroscience Abstracts **31**: 668.
- Zsombok, A. and K. M. Jacobs (2007). "Postsynaptic Currents Prior to Onset of Epileptiform Activity in Rat Microgyria." J Neurophysiol **98**(1): 178-186.

Vita

Nicole Ekanem was born in Northern Virginia and lived there until she moved to Richmond, Virginia in 2008 to start university. Little did she expect to end up staying in Richmond for this long...